A DEFORMATION ANALYSIS OF THE SEEPAGE CUTOFF WALL AT MUD MOUNTAIN DAM, WASHINGTON

By

E. WAYNE KUTCH

Bachelor of Science

University of Washington

Seattle, Washington

1979

Submitted to the Faculty of the Graduate College
of the Oklahoma State University
in partial fulfillment of the requirements
for the Degree of
MASTER OF SCIENCE
May, 1991

A DEFORMATION ANALYSIS OF THE SEEPAGE CUTOFF WALL AT MUD MOUNTAIN DAM, WASHINGTON

Thesis Approved:

Thesis Adviser

Dean of the Graduate College

PREFACE

A seepage cutoff wall being installed at Mud Mountain Dam, Washington, was analyzed by means of a two-step process. Load-deformation characteristics of the embankment were first established using finite element techniques in conjunction with a range of assumed soil parameters. The computed load-deformation soil response characteristics were then utilized as supports in a grid structure model of the wall to predict deformations and stresses.

It is hoped this exercise will provide a means of evaluating data obtained from monitoring instrumentation to be installed at the project. It should also be useful in the evaluation of similar installations and therefore have some potential application in the design of such. The diaphragm wall as a method of controlling seepage in embankment dams has only recently been gaining acceptance in this country and information on the analysis of these structures is still relatively scarce. However, with the great number of dams in the United States which are in need of remedial action, it is important that a suitable method for their analysis be developed. The methodology utilized in this analysis provides a possible approach to this problem and may be suitable for many applications.

My sincere appreciation is expressed to the individuals who assisted me in this undertaking: In particular, Dr. William P. Dawkins, for providing direction and assistance throughout its preparation; my super-

visor, Paul Noyes, for his support and intelligent advice when it was needed; Mike Nelson, Mud Mountain Dam Rehabilitation Project Engineer, and Gerrett Johnson, Assistant Chief, Design Branch, both of the Seattle District U.S. Army Corps of Engineers, who went out of their way to provide support for my undertaking this study; and Professor Joseph Kaushchinger of Tufts University for his expertise and invaluable assistance regarding soil modeling techniques.

TABLE OF CONTENTS

LIST OF TABLES

LIST OF FIGURES

CHAPTER I

INTRODUCTION

This study describes a deformation analysis of the seepage cutoff wall recently installed at the Mud Mountain Dam Project. Mud Mountain, located on the White River near Enumclaw, Washington (Figures 1 and 2), is a rockfill dam with a rolled earth core. It has a maximum embankment height of 425 feet and a crest length of 700 feet. Construction of the dam began in 1939 and was largely complete when interrupted by the war effort in 1941. It did not become fully operational until 1949. The project is owned by the United States government and is maintained by the U.S. Army Corps of Engineers. A typical section of the dam is depicted in Figure 3.

The cutoff wall installation was undertaken in response to concern regarding the integrity of the dam core, prompted by indications of excessive seepage through the embankment. The seepage was first detected through correlation of piezometer response to pool fluctuations in 1976. Subsequent site investigation yielded evidence of deterioration to the dam core, including loose zones, voids, and cracks, as well as an apparent loss of fines.

After ten years of monitoring and investigation, it was determined in 1986 that remedial action would be necessary. A study of potential repair methods led to the selection of a diaphragm cutoff wall as the most suitable seepage control measure for the site. Due to the scarcity

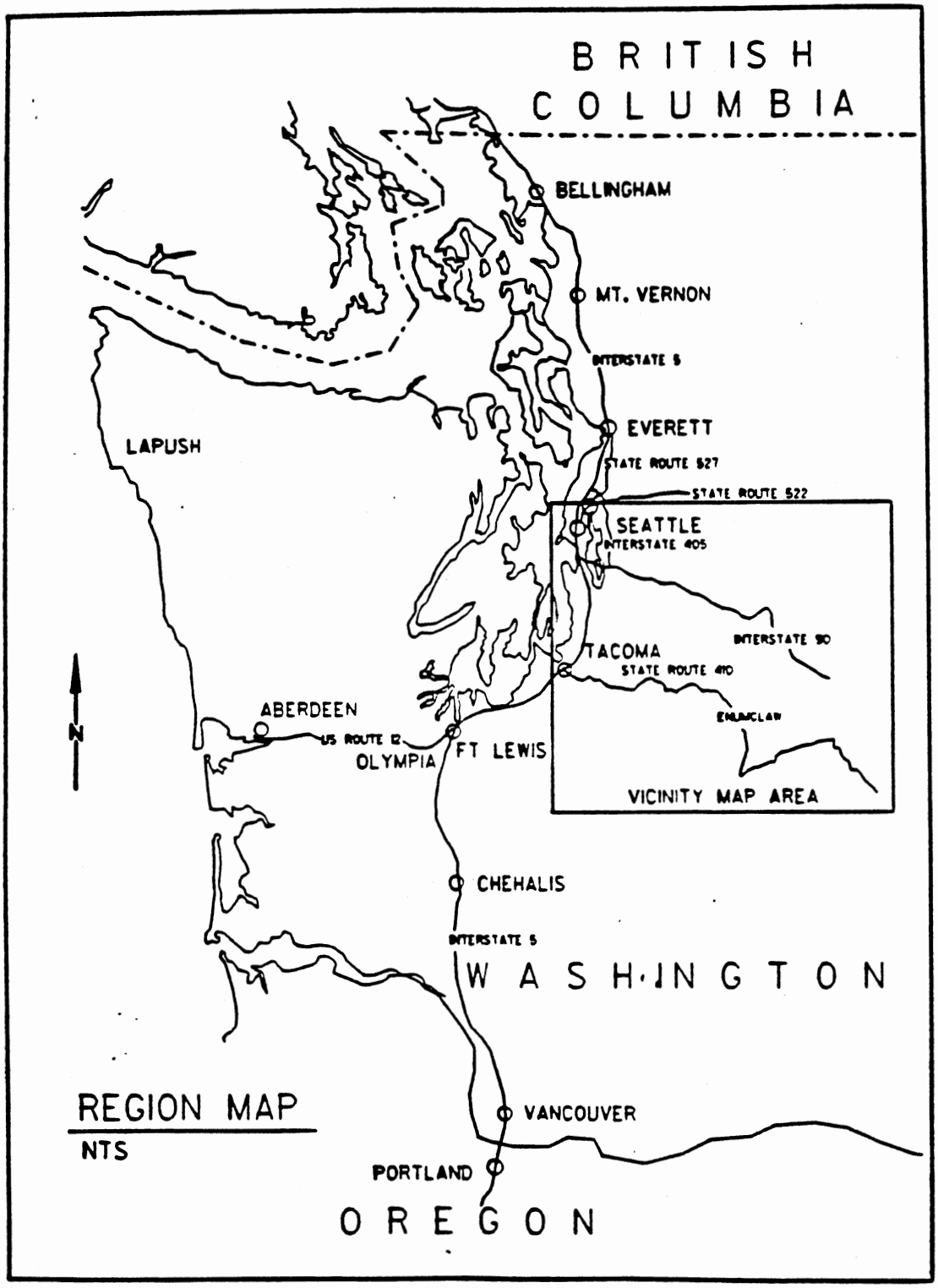

Figure 1. Region Map

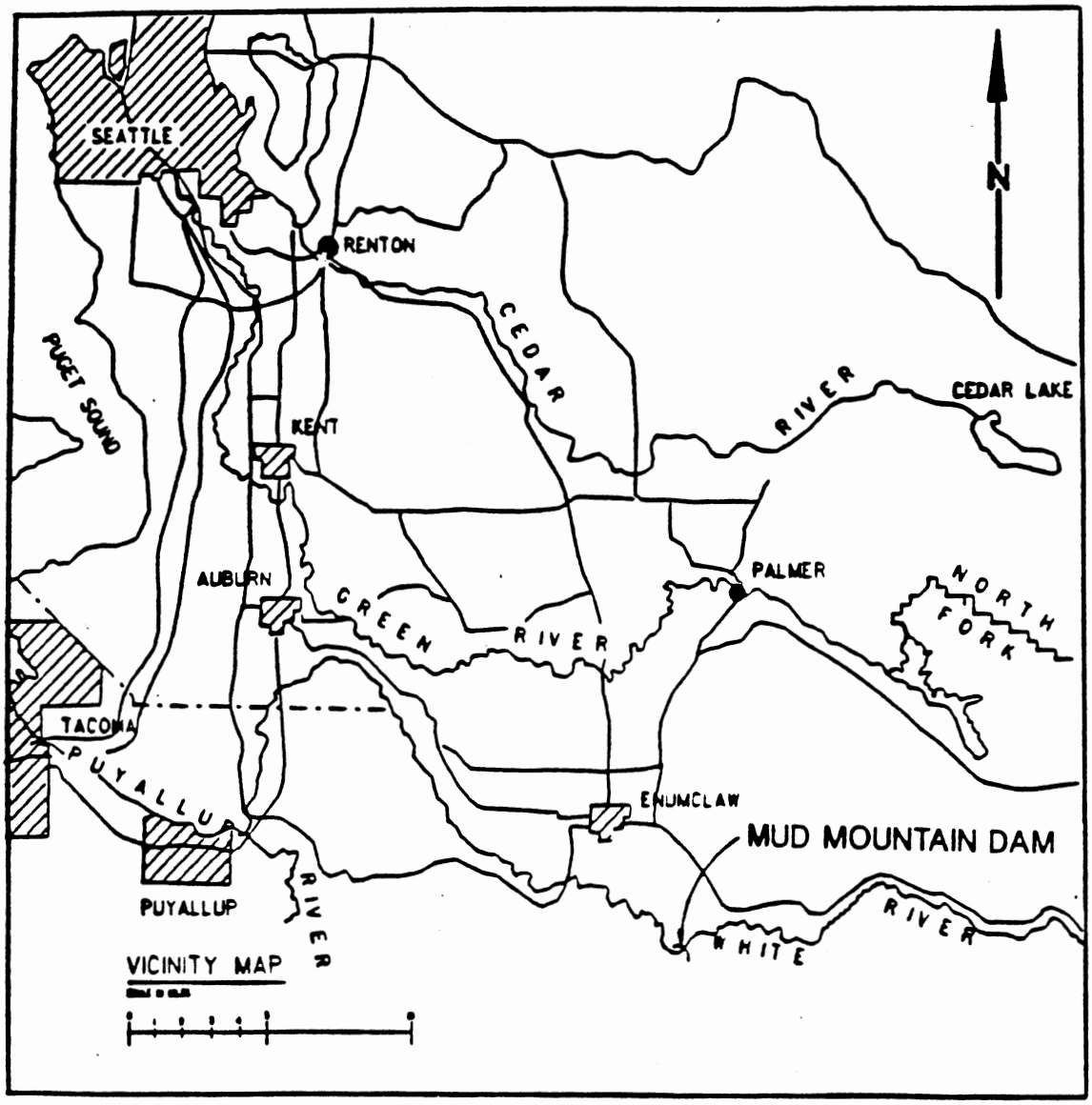

Figure 2. Vicinity Map

MUD MOUNTAIN DAM

TYPICAL SECTION

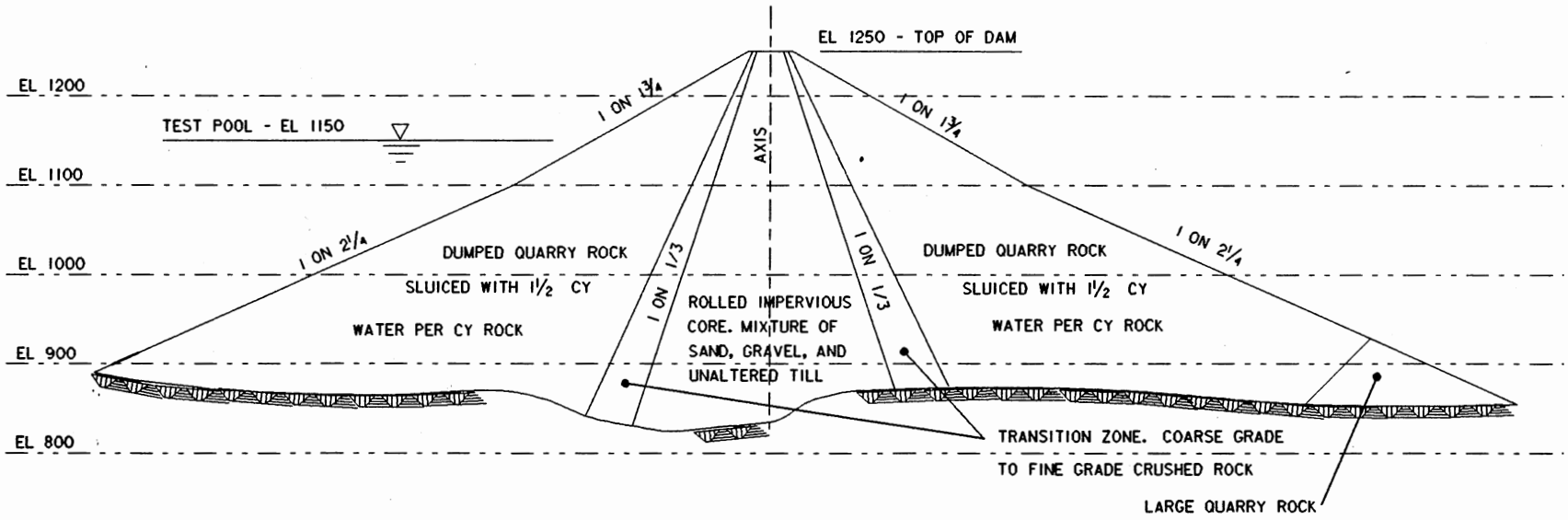

Figure 3. Dam Embankment Cross Section

of design-related information on this type of installation, the plans relied heavily on data obtained from similar cutoff wall installations. The original analysis was accomplished utilizing the SAP5 [12] finite element analysis computer program and the Corps program CBEAMC [1]. The plans called for the installation of a wall extending the full height of the embankment and keyed a minimum of 15 feet into the rock abutments and foundation. Wall thickness is either 24 or 40 inches, depending on location in the embankment.

Although the original design analysis was considered sufficiently accurate to proceed with plans and specifications, expediency required the use of several simplifying assumptions pertaining to soil stress-strain behavior and perimeter support conditions. The purpose of this study is to provide a more comprehensive analysis of this installation.

The cutoff wall consists of unreinforced concrete with a minimum compressive strength of 3000 psi. The wall is constructed of a horizontal line of 67 individually placed sections, each of which extends the full height of the embankment from foundation rock to the dam crest. Panel widths range up to a maximum of 23 feet with a maximum thickness of 40 inches. The panels extend into the foundation rock a minimum distance of 15 feet to provide a sufficiently long path around the wall perimeter in order to minimize seepage. The standard construction sequence requires placement of 22-foot wide "primary" panels with a clear separation of approximately 8 feet. After the primary panels are cured for one to two weeks, intermediate "secondary" panels are installed. During secondary panel excavation, the cutter head not only removed earth but bites 12 inches into the adjacent primary panels, a procedure designed to promote concrete bond strength development at the joint.

In the research effort described herein, an attempt has been made to account for the perceived physical characteristics of such a structure and potential effects caused by variations in soil support characteristics.

CHAPTER II

PREVIOUS RELATED RESEARCH ON DIAPHRAGM WALLS

The diaphragm wall as a remedial measure to seepage in embankment dams has only recently been gaining acceptance in this country, although it apparently has been used in Europe with appreciable success. Research on these installations is correspondingly sparse and there are no established analysis procedures being used at this time. The following summaries describe research that was found to be useful in the preparation of the Mud Mountain analysis which is the subject of this study.

Finite Element Method

A description of a finite element approach to cutoff wall analysis is presented in the Bureau of Reclamation Technical Memorandum FO-230-5 [2] concerning an installation at Fontanelle Dam in Wyoming. The embankment height of Fontanelle is approximately 150 feet, less than one-half of that at Mud Mountain. In both cases the wall is fully keyed into a weathered rock foundation around the perimeter.

The two-dimensional finite element model of the dam used in the analysis is taken perpendicular to the axis of the dam and consists of a total of 350 elements. Included in the model are elements representing the dam core, shell, foundation, and the cutoff wall. Upper and lower bound modular values for the dam core material were approximated from test results performed on soil taken from the borrow area. Shell and

foundation properties were estimated based on the results of tests on similar materials.

The results of the analysis indicate a maximum displacement of the wall of 3.12 to 8.45 inches. The effects of upper and lower bound core modular values were considered, as well as the effects of variation in the modulus of cutoff wall concrete. The core material modulus was found to have a much greater influence on displacements than concrete wall element strength. Stresses in the concrete wall were found to be closely related to the secant modulus and allowable tensile strength of the concrete.

Beam on Elastic Foundation

A generalized approach to cutoff wall analysis utilizing a beam on elastic foundation theory is described in the Bureau of Reclamation technical memorandum entitled "Deformation Analysis of a Diaphragm Wall" [3]. An illustration of this approach, based on the cutoff wall at Navajo Dam, is included in the memorandum. The physical characteristics of the Navajo Dam provided in the report include an embankment height of 220 feet and an overall wall height of 360 feet, indicating that the wall is keyed very deeply into the dam foundation. The wall thickness of 32 inches is less than the 40-inch thickness typical of the deeper portions of the Mud Mountain installation, while the specified minimum concrete compressive strength of 4000 psi is greater.

In the beam on the elastic foundation approach, the deflected shape of the wall represents a position of equilibrium between a driving force and resistive force. The driving force consists of the sum of the hydrostatic pressure and the active earth pressure on the upstream face of

the wall. Resistance to the driving force is furnished by the passive earth pressure acting on the downstream face of the wall. The downstream reaction in this case is the sum of the coefficient of the horizontal subgrade reaction, k_h, multiplied by displacement; and a p_o' value which accounts for the variation in soil resistance as a function of depth. The k_h values of 20 and 40 kips per cubic foot used in the Navajo analysis represent medium and high values, respectively, for flexible retaining structures in sand.

The results of this analysis indicate a maximum displacement ranging between 0.5 and 3.9 inches, depending on which value of k_h was used and which of the five applied pressure distributions included in the study is assumed. No attempt was made in this study to evaluate the stress condition in the wall corresponding to the computed deformations.

Instrumentation Report

A report describing the instrumentation results of a monitoring program implemented at the Manicougan 3 Dam in Quebec, Canada, is also of interest in the Mud Mountain analysis. The Manicougan 3 cutoff differs from the Mud Mountain installation in that it provides seepage control to the dam foundation rather than the embankment and is an integral part of the dam installation as opposed to a remedial effort. At 420 feet, the Manicougan 3 cutoff is similar in height to the Mud Mountain installation and is similarly situated in a deep, narrow canyon. As a foundation cutoff, however, it penetrates primarily into the dam foundation and extends only partially into the embankment. Significant settlement and associated skin friction effects were anticipated for this

installation, resulting in the use of a pair of adjacent diaphragm walls to reduce axial stresses.

The inclinometer data for the Manicougan cutoff indicate a maximum downstream displacement of approximately 11 inches, occurring at the top of the wall, with intermediate displacements nearly proportional to the distance up the wall. Although the deformed shape of the wall differs from the predicted deformed configurations in the previously described Fontanelle and Navajo analysis, the location of maximum displacement as a proportion of the embankment height appears to be similar.

Comments on Related Research

A summary of both analysis methods provides a logical method of approaching the problem of cutoff wall behavior in a continuous medium. However, as the structure width decreases relative to structure height, the effects of constraint along vertical portions of the wall perimeter become correspondingly more significant, an effect not accounted for in either of the analysis methods described. A possible method of accounting for these effects would be by means of a three-dimensional finite element analysis. This approach, however, tends to be time-consuming and costly, requiring the development of a large and complex model. In the case of the Mud Mountain installation, it was therefore desirable to develop an economical method of modeling the wall-soil system that would still account for the influences of perimeter constraints. Also desired was a more comprehensive evaluation of potential magnitudes and distribution of stress levels in the cutoff wall. Although concrete stress is addressed in the Fontanelle analysis, a more thorough understanding of

the effects of joints and perimeter constraints on wall behavior will be useful in future designs.

CHAPTER III

FINITE ELEMENT MODELING

Analysis Approach

The dam embankment was modeled using a two-dimensional plane-strain finite element model of the dam, oriented perpendicular to the axis of the dam, consisting of 146 nodes and 133 elements (Figure 4). Properties for both core and rock shell material were developed and hydrostatic forces were applied directly to the element nodes. The model was then analyzed by means of the structural analysis program GSTRUDL [11]. Load-deformation relationships at the wall location were developed from the computed nodal displacements and utilized for support springs in a planar grid structure model. The grid was analyzed using the structural analysis program CGRID [5] to determine moments, shears, and deformations in the concrete cutoff wall.

Determination of Soil Moduli

The load-deformation behavior of soils is highly complex and may depend on a number of factors including density, water content, structure, drainage conditions, duration of loading, stress history, confining pressure, and shear stress. Despite this wide variety of influences, it is often necessary to quantify this behavior for problems such as those encountered in the effort reported herein. Recent work has indi-

MUD MOUNTAIN DAM

FINITE ELEMENT MODEL

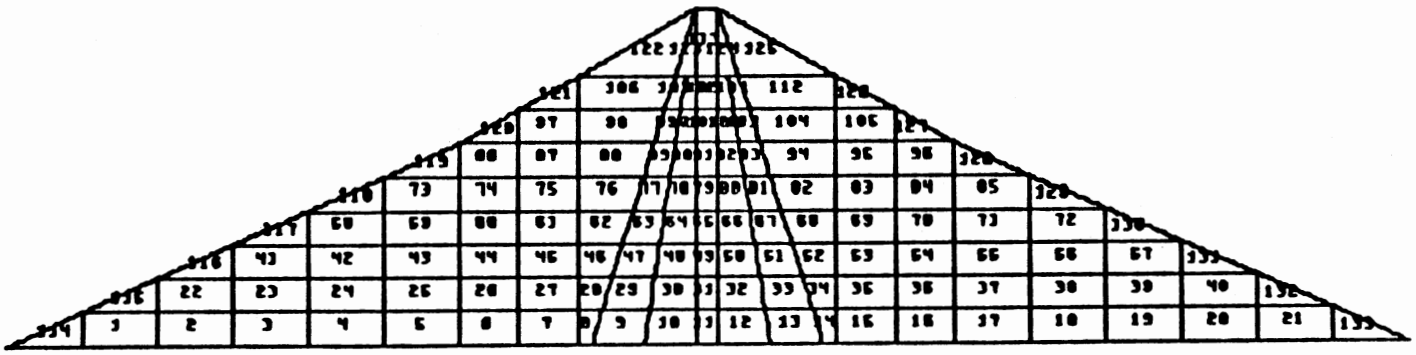

Figure 4. Dam Embankment Finite Element Model

cated that the stress-strain behavior as suggested by triaxial tests can be represented by the following relationship [6,7,8]:

$$(\sigma_1 - \sigma_3) = \frac{\varepsilon}{\frac{1}{E_i} + \frac{\varepsilon}{(\sigma_1-\sigma_3)_{ult}}} \tag{1}$$

where $(\sigma_1-\sigma_3)$ is the deviator stress, which is the difference between principal stress and confining pressure; and E_i is the initial tangent modulus of the soil at a particular confining pressure, σ_3. $(\sigma_1-\sigma_3)_{ult}$ is called the asymptotic stress difference and can be determined by the equation

$$(\sigma_1 - \sigma_3)_{ult} = \frac{(\sigma_1-\sigma_3)_f}{R_f} \tag{2}$$

where R_f is a dimensionless coefficient called the failure ratio, and

$$(\sigma_1 - \sigma_3)_f = \frac{2c\cos\phi + 2\sigma_3 \sin\phi}{1 - \sin\phi} \tag{3}$$

in which c and ϕ are the cohesion intercept and the friction angle for the soil, respectively. The initial tangent modulus can be determined by the equation

$$E_i = K\, p_a \left(\frac{\sigma_3}{p_a}\right)^n \tag{4}$$

where K and n are dimensionless parameters termed the modulus number and modulus exponent, respectively; and p_a is atmospheric pressure in the same units as E_i.

Attempts at standardizing this approach have led to the evaluation of at least 150 different soils for the parameters K, N, c, ϕ, and R_f, to be used in the preceding equations [6,8]. It was therefore possible, for the purpose of this study, to select representative parameters for

the core and shell from the tabulated results of such testing, based on similarities (gradation, unit weight, etc.) to the actual embankment materials.

Embankment Parameters

In order to determine the relative contributions of both core and shell to the model behavior and determine the sensitivity of the model to these parameters, wall behavior was investigated using soil parameters corresponding to two types of core and shell materials. Core material parameters investigated correspond to samples taken from the Round Butte Dam core and the Binga Dam Core, and were both selected based on their physical similarity with the Mud Mountain Dam core material. The hyperbolic stress-strain curves for both dam core materials are compared in Figure 5. The confining pressure, σ_3, of 10 ksf which was used to develop the plot, corresponds to a depth of approximately 150 feet in the embankment. The Round Butte Dam core material is considerably stiffer than the Binga Dam core material, as indicated in Figure 5 by the steeper slope of its curve.

The two sets of parameters selected to represent the behavior of the Mud Mountain shell correspond to a diorite rockfill and a conglomerate rockfill. Although the material used to develop these parameters consisted of a finer gradation than the large rock in the Mud Mountain shell, both are comparable in terms of void ratio and internal friction angle. A graph of the hyperbolic stress-strain curves for these materials is presented in Figure 6, from which it may be seen that the conglomerate rockfill is stiffer than the diorite rockfill.

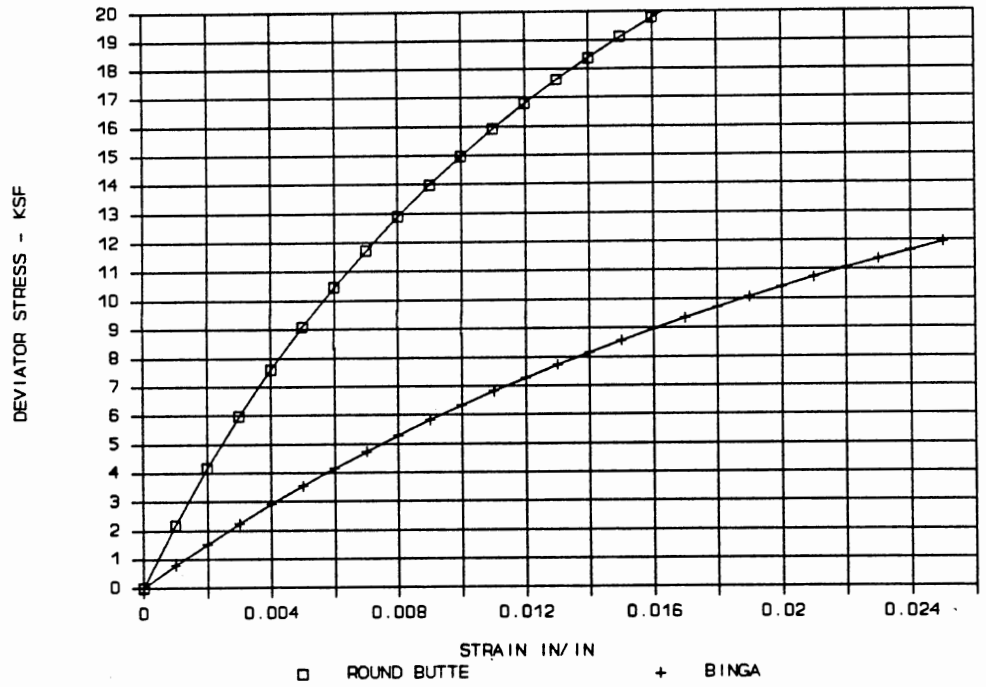

Figure 5. Dam Core σ-ε at 10 ksf Confining Pressure

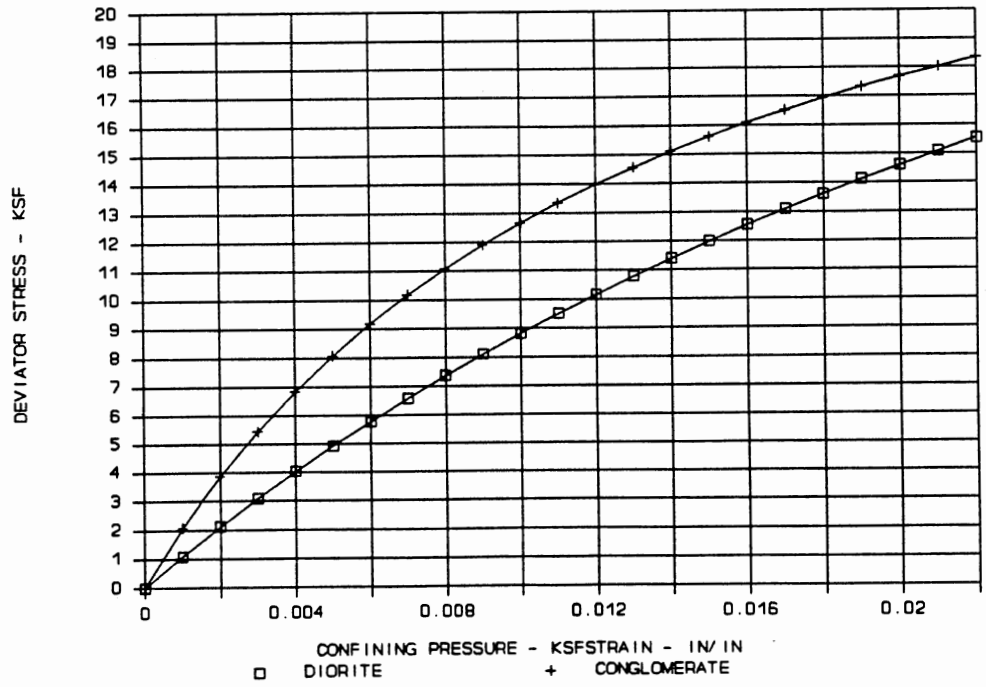

Figure 6. Dam Shell σ-ε at 10 ksf Confining Pressure

Figure 7 shows a comparison between a hyperbolic stress-strain curve and initial tangent modulus for the Round Butte Dam core material at an assumed confining pressure of 10 ksf. As this figure illustrates, the linear and hyperbolic functions are approximately coincident for very small strains. This similarity was utilized in the effort reported herein to allow the use of linear finite element behavior. Since the two functions diverge with increasing strain, it was necessary for each set of material parameters to assess the significance of such divergence on the results obtained. The method and results of this assessment will be addressed elsewhere in this study. Graphs of the initial tangent modulus as a function of confining pressure for both core and shell materials are shown in Figures 8 and 9.

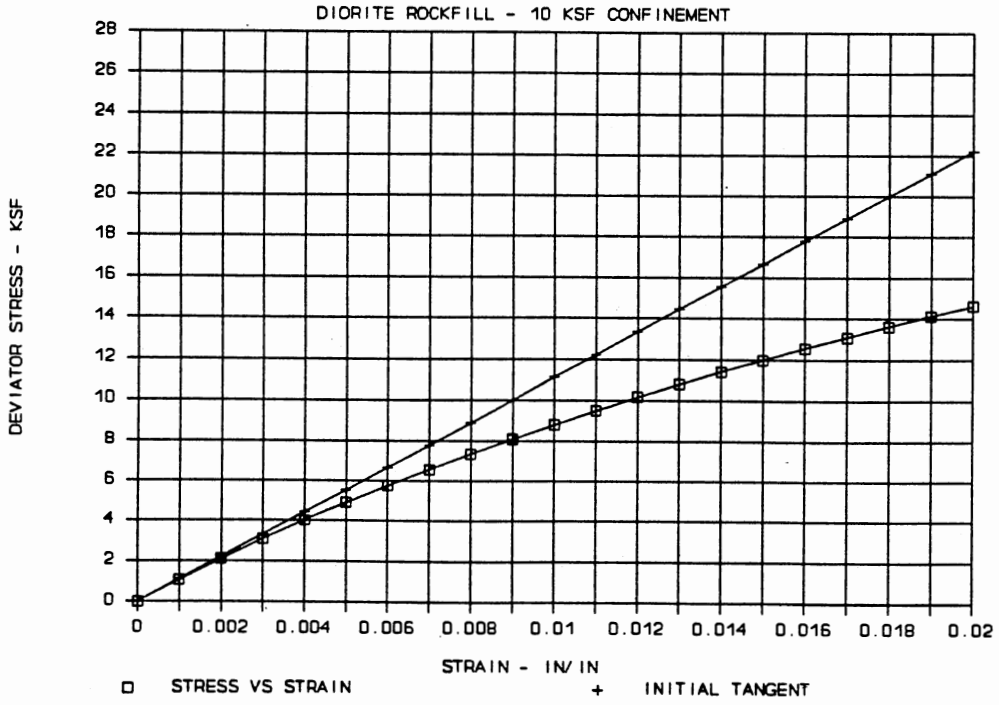

Figure 7. Round Butte Dam Core--Actual Vs Initial Tangent Modulus

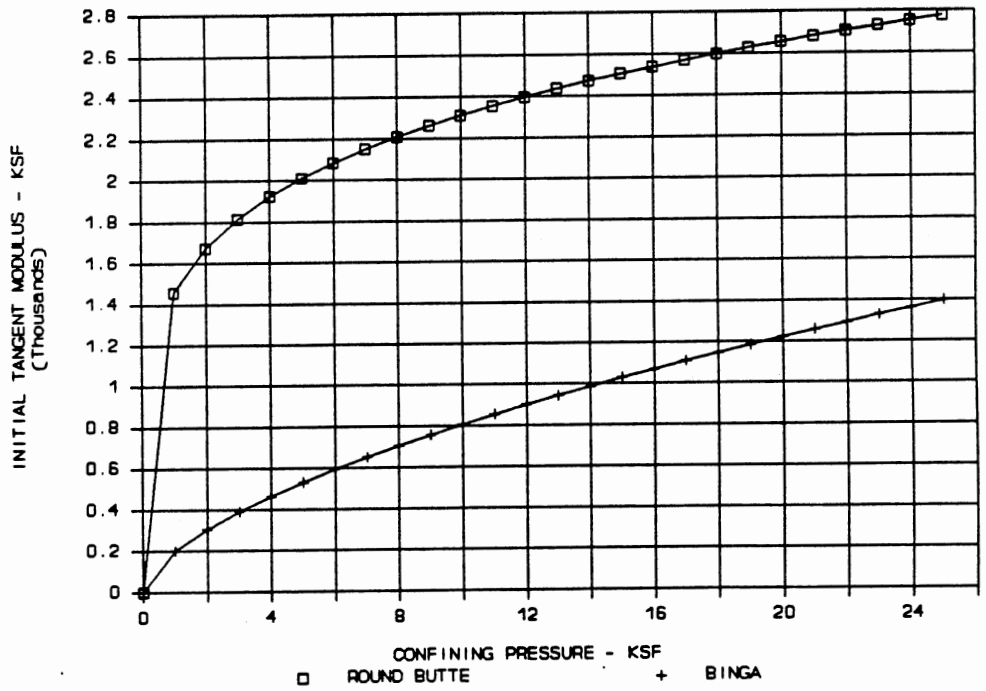

Figure 8. Dam Core--Initial Tangent Modulus Vs Confining Pressure

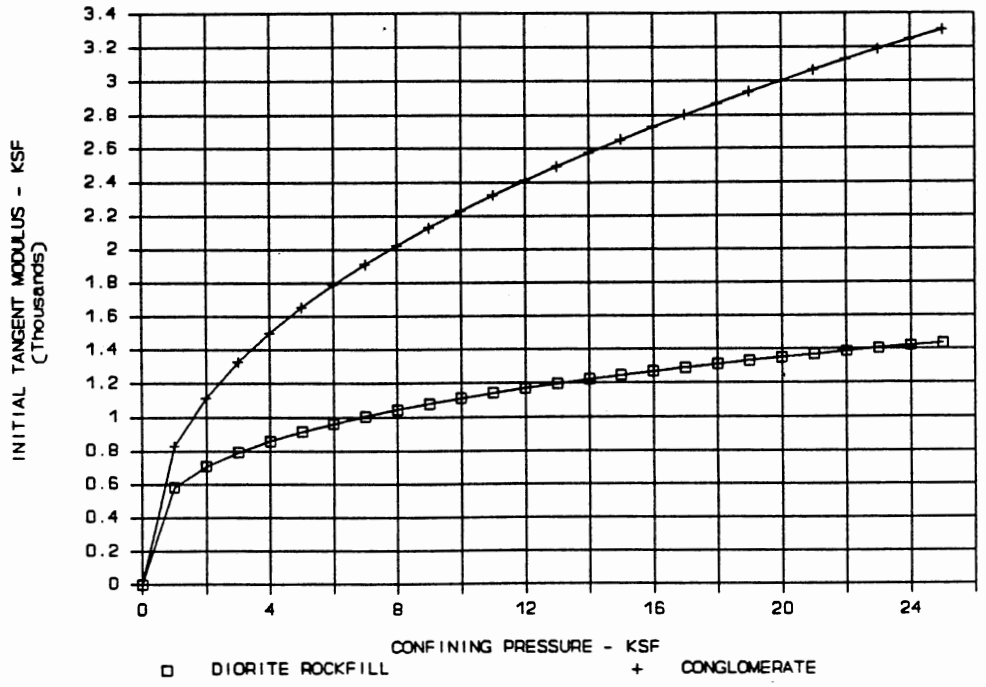

Figure 9. Dam Shell--Initial Tangent Modulus Vs Confining Pressure

Sign Convention

The sign convention used for this exercise is positive for downstream displacements and positive for (passive) soil pressure acting to resist downstream displacements (Figure 10).

Soil Behavior Modeling

According to the designated sign convention, displacement of the cutoff wall will be in the positive direction when hydrostatic forces are applied. Prior to wall displacement, the at-rest soil pressure will be acting on the downstream face of the wall in the positive direction. In response to positive wall displacement, this pressure will increase as passive resistance is mobilized in the soil. The rate at which passive resistance is developed is expressed by the soil modulus, which, as already indicated, is approximately linear for small strains. In the finite element model used in this analysis, the at-rest pressure coefficient, K_o, of 0.5 is reproduced by assigning a Poisson's ratio of 0.33 to the elements. Resistance of the downstream soil elements to lateral deformation in the model is slightly higher than the soil modulus would suggest. This occurs as a result of the conditions of strain compatibility in the two-dimensional plane-strain model. The magnitude of the increase in the effective soil modulus produced by this condition was found to be approximately 11 percent and does not constitute a significant variation relative to the degree to which soil parameters are known.

On the upstream face of the cutoff, soil pressure will act in a negative direction and will change from at-rest to active as positive displacement occurs. The corresponding soil elements in the finite

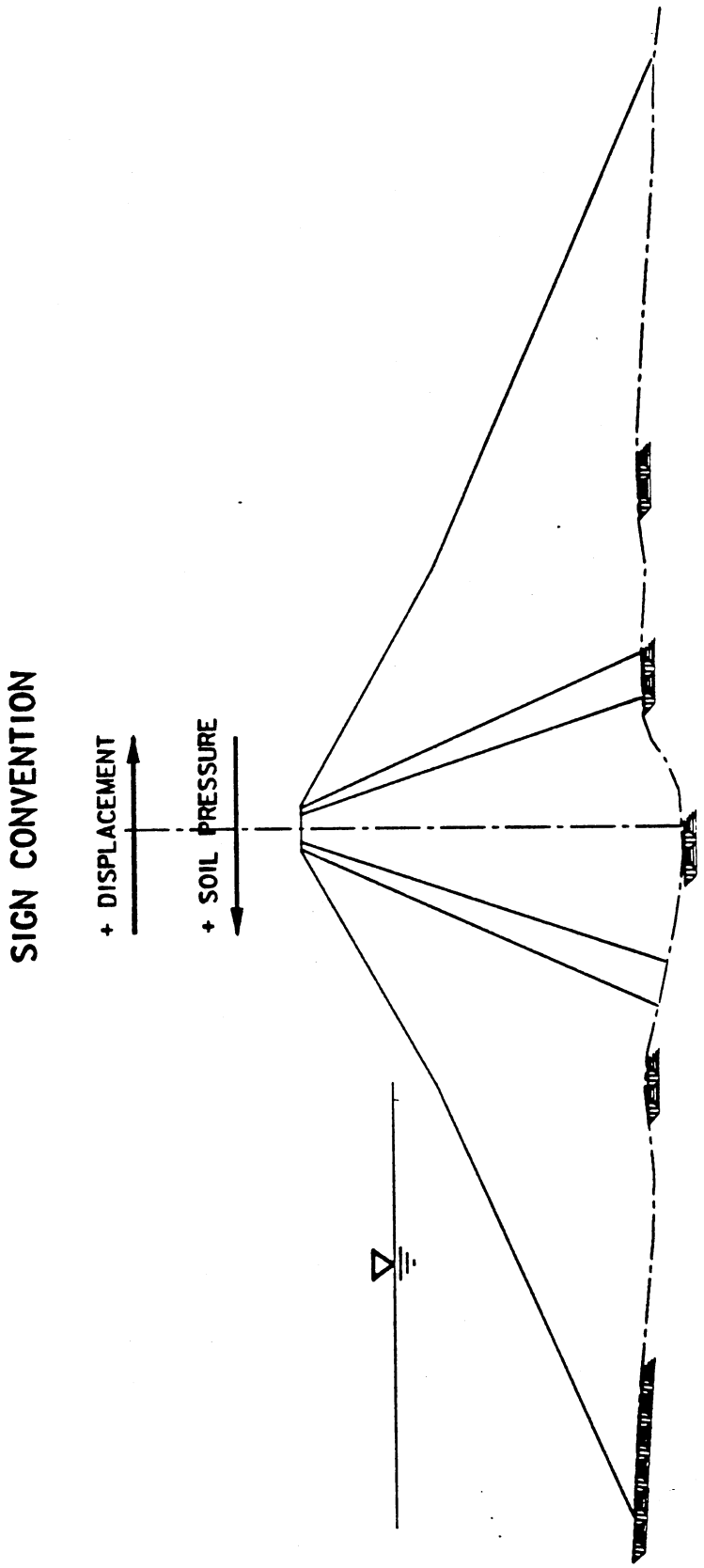

Figure 10. Sign Convention

element model exhibit positive strain (elongation) under the conditions. A corresponding decrease in horizontal stress takes place in the upstream elements, which are initially in compression due to Poisson's effect. In the case of actual soil behavior, lateral soil pressure may decrease only until the full active limit state is achieved, at which point additional displacement yields a constant lateral pressure. However, in the linear finite element program used in this analysis, this limitation could not be accounted for in the input stages. It was therefore necessary to verify that the calculated horizontal stresses were within the acceptable range for active soil pressure. The magnitude of full active pressure is expressed by the product of the active pressure coefficient, K_a, and the vertical pressure, and is a function of the embankment geometry and material characteristics. For the sloping dam embankment geometry, the active pressure coefficient is expressed by the equation

$$K_a = \left[\frac{\cos\phi}{1 + \sqrt{\sin\phi\ (\sin\phi + \cos\phi\ \tan\delta)}}\right]^2 \qquad (5)$$

where δ is the angle of the embankment measured from the horizontal, and ϕ is the internal angle of friction of the embankment material. In the case of Mud Mountain Dam, active behavior is thought to be primarily governed by the rock shell, for which the average internal friction angle is estimated to be approximately 45 degrees. Using Equation (5), the value of K_a was determined to be between 0.13 and 0.14, depending on elevation. The requirement that the computed horizontal stress at least equal the product of this factor and the indicated vertical stress at any point provided the verification of the validity of the program results in positive strain regions. As in the case of passive resistance,

soil behavior was assumed to be linear and no adjustment to soil modulus values was made to account for strain compatibility effects.

Loading Condition

The loading condition assumed in this analysis was a hydrostatic pressure distribution corresponding to a pool elevation of 1150, which approximates the highest pool of record at the project. Loads were applied as concentrated forces at the element nodes in both the finite element and grid structure models.

Finite Element Results

The results of the finite element analysis indicate that deformations are controlled primarily by the rock shell parameters. Maximum calculated deflection using the conglomerate rockfill shell was 12.1 inches at nodes 75 and 92, using either of the core material parameters. This maximum displacement occurred at depths of 280 and 240 feet in the embankment, or approximately two-thirds the overall depth of the embankment. Differences between nodal displacements using Round Butte core parameters as opposed to Binga core parameters were generally less than 0.1 inch.

For the case of the diorite rockfill shell, the maximum nodal displacement increased to approximately 19 inches, also in the 280- to 240-foot depth range. Once again the difference in displacement between the two core materials was found to be insignificant. The surprisingly small influence of the core material parameters in the model behavior is thought to be caused by the relatively short horizontal soil column this material provides compared to the large rock shell cross section (Figure

3). A comparison of the deformed shapes of the cutoff wall utilizing the two different rockfill shell parameters is shown in Figure 11.

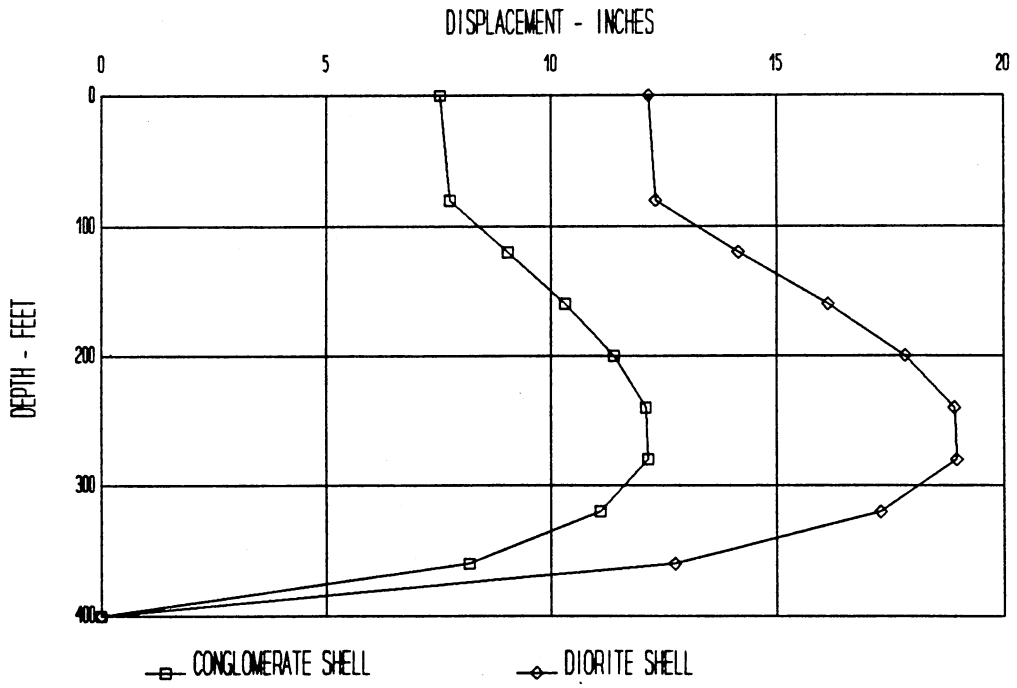

Figure 11. Displacement Vs Depth

Verification of Finite Element Results

As previously indicated, verification of the finite element results was necessary, particularly in areas of relatively high strains. These areas are primarily located in the dam core adjacent to the cutoff wall. For the case of negative strains, indicating mobilization of passive resistance, verification required determination of the degree of divergence of the theoretical hyperbolic model from the initial tangent

modulus. A maximum negative strain of 0.00139 occurs in the core at element 31 using the lower modulus diorite shell parameters. This corresponds to a deviator stress of 3.347 ksf according to the initial tangent modulus of 2408 ksf used by the program for this element, compared to a theoretical value of 3.146 ksf given by Equation (1), a divergence of approximately 6.4 percent. Since the average negative strain throughout the model is considerably less than occurs at element 31, the overall contribution of such divergence does not appear to constitute a significant source of error for the effort reported herein.

For the case of positive strains, valid results required that lateral pressure not fall below the minimum value for active behavior as given by Equation (5). This requirement was met at all locations, with the exception of several nodes at the base of the transition elements 123 and 124 (see Figure 4). These exceptions are not significant since they occur in an area of very low stress and are above pool level.

Effect of Preload

The procedure used in installing diaphragm cutoff walls may introduce significant deviator stresses into the embankment during construction. Each panel is constructed by first excavating into the embankment using a specially developed cutter, called a hydrofraise, mounted on a crane. Excavation is taken to the full depth of the panel; the trench sidewalls are supported by a bentonite slurry mixture which is maintained at a level 10 feet from the top of the trench. The purpose of the slurry is to prevent sloughing of the trench, by equalizing the lateral soil pressures. Optimally, any tendency for the slurry to migrate into the surounding embankment is prevented by the "sealing"

capability of the bentonite. The unit weight of the bentonite slurry is approximately 65 pcf, which approximates the lateral earth pressure of the embankment. After excavation has reached the required depth, the concrete panel is placed by pumping concrete into the trench, displacing the slurry. The unit weight of the concrete, at around 150 pcf, produces considerably greater lateral pressure than the bentonite slurry while in a fluid state. This lateral pressure is controlled by the concrete placement rate and rate of slump loss. These factors at the Mud Mountain project indicate the potential for as much as 100 feet of fluid concrete or 15 ksf maximum lateral pressure. This concrete fluid pressure is partially equalized by the at-rest soil pressure, producing a maximum deviator stress of approximately 8 ksf. This stress is exerted on both sides of the panel, acting in a positive (upstream) direction on the upstream side of the trench and a negative direction on the downstream side of the trench. The resulting passive soil pressure thus mobilized would theoretically still be present in the soil after the concrete sets up and before any pool load is applied.

The potential effect of the soil preload on the overall structure can be explained by referring to Figure 7. The applied deviator stress will compress the soil on opposite sides of the trench, corresponding to a point away from the origin on the soil stress-strain curve for each elevation. Since the concrete sets up while exerting lateral force, the point thus attained on the curve becomes essentially a new initial condition on which hydrostatic pool loads will act. In the case of the embankment on the downstream side of the cutoff wall, pool loads act in the same direction (downstream) as the preload. Downstream displacement of the wall will be resisted by mobilization of passive resistance of

the soil, according to a rate governed by the modulus at the "new" area on the stress-strain curve attained by the initial preload. The hyperbolic configuration of the stress-strain curves indicates the resulting modulus thus attained will be lower than the initial modulus.

In the case of the Round Butte core material, using a deviator stress of 8 ksf and a depth in the embankment of 260 feet, the resulting modulus reduction amounted to 30 percent. However, on the upstream side of the cutoff wall, the downstream displacement of the wall due to the applied pool load that will occur acts in an opposite direction as the initial preload, thus relieving the stresses previously mobilized. This effect is significant in that triaxial testing of soils indicates the soil that has been initially loaded exhibits markedly higher modulus behavior under unloading-reloading conditions [6,7,8]. Such testing suggests that the modulus under these conditions typically ranges between 1.2 and 3.0 times the initial modulus value. The result is that the initially balanced soil pressures mobilized by the preload will decline at a much faster rate on the upstream side of the wall (acting downstream) than would otherwise occur without the effect of the initial preload. It is therefore seen as significant in terms of cutoff wall behavior that the combined modulus of the two soil masses is actually increased. However, a quantified assessment of this effect requires the use of numerous assumptions (unloading-reloading modulus to initial modulus ratio, zone of influence of the preload, deviator stresses, etc.) and is considered beyond the scope of this investigation.

CHAPTER IV

GRID STRUCTURE ANALYSIS

General

Force and deformation response of the concrete cutoff wall was evaluated using a planar grid model of the wall-soil system. Embankment characteristics determined from the finite element model were then incorporated into the grid as interior support springs. Support conditions at the grid perimeter were also developed to approximate the constraint along the cutoff wall interface with both rock and overburden. Moment continuity was assumed throughout the model for the initial analysis, corresponding to an uncracked wall. Additional analysis was also performed considering the effects of flexural overstressing at the vertical cold joints between adjacent panels. The loss of flexural resistance resulting from cracking at these locations was simulated in the analysis by the release of bending force about the vertical axis.

Grid Configuration

The configuration of the rock canyon at the cutoff wall location is shown in Figure 12. This geometry was approximated by the grid model shown in Figure 13, which consists of 100 nodes and 159 elements. Node spacing was reduced at greater depths, as well as along the rock-wall interface, since these areas are typically associated with higher stress levels and therefore warrant a higher level of detail.

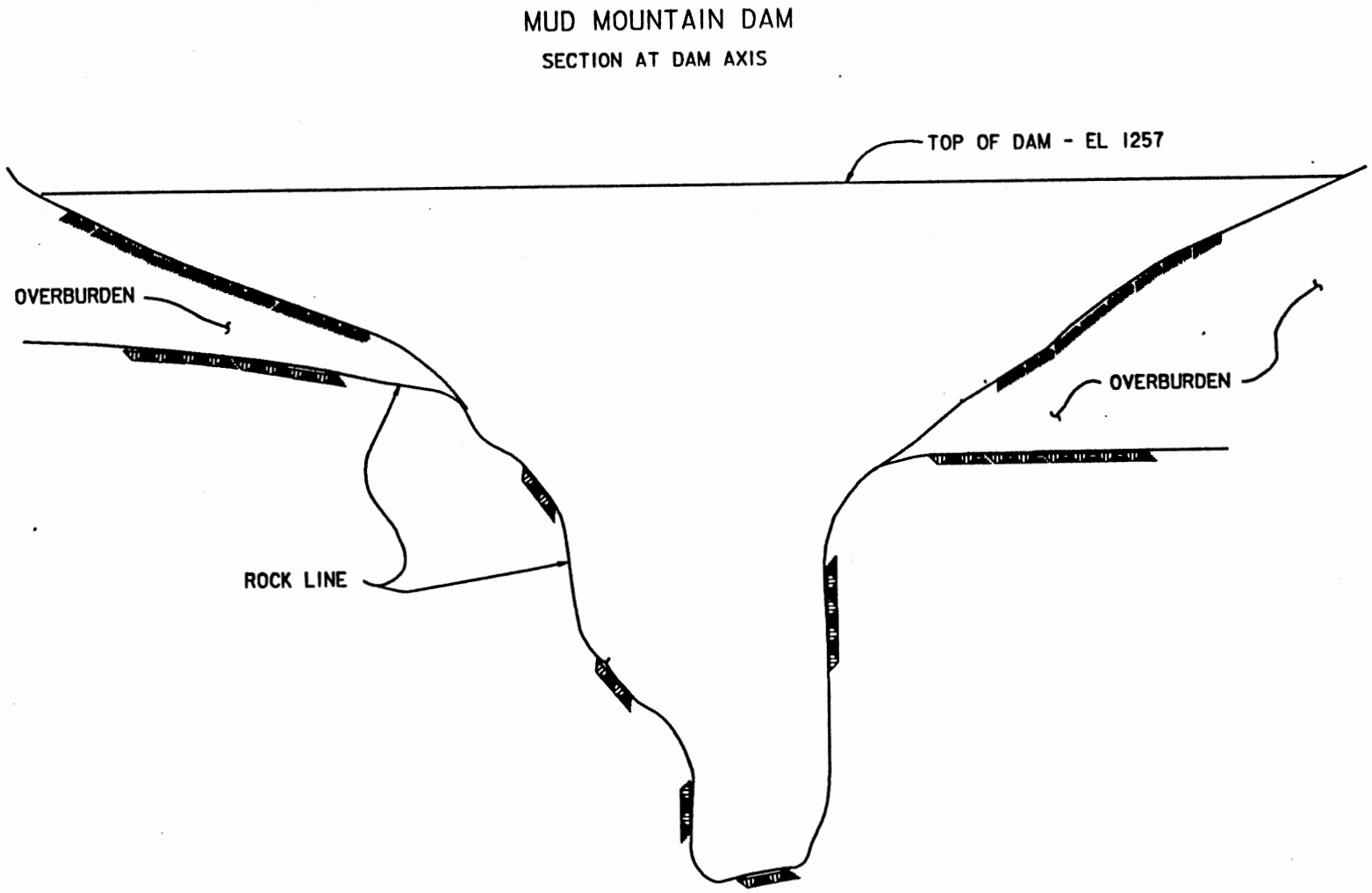

Figure 12. Cross Section at Dam Axis

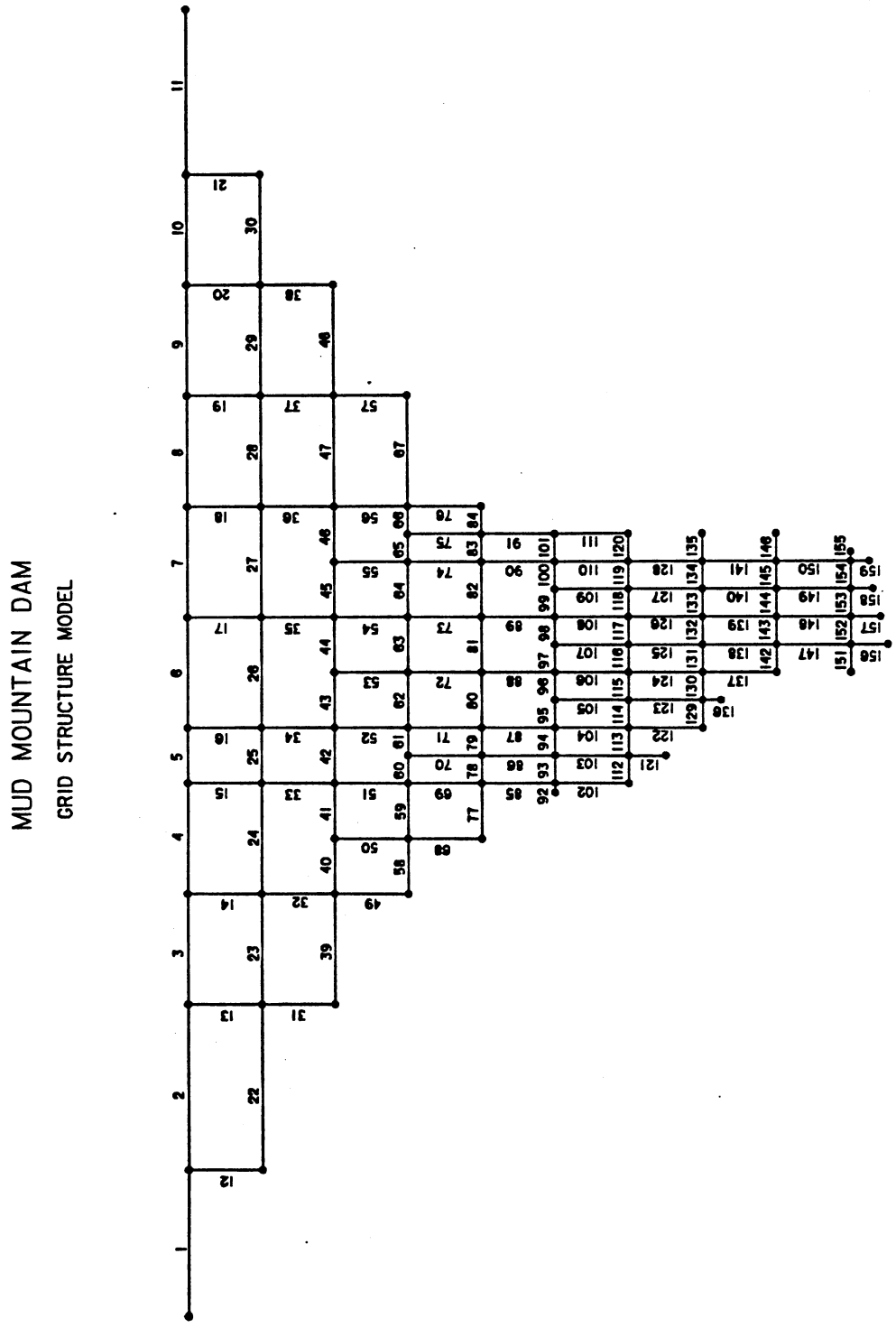

Figure 13. Grid Structure Model

Element Properties

Element dimensions were determined by tributary area and provided as input for property computation by the program CGRID. The modulus of elasticity of the concrete was determined from the ACI code equation, $57000\sqrt{f'_c}$, which produces a value of 3122 kips per square inch for the 3000 psi minimum compressive strength required by the contract specifications.

Interior Support Springs

Spring constants at interior nodes representing the deformational resistance of the dam embankment were determined from the finite element results. The concentrated loads used in the finite element model were converted to unit loads according to tributary areas and then compared with the resulting deformations. The results of this comparison for both the diorite and conglomerate rockfill shells were then plotted as a function of depth in the embankment, as shown in Figure 14. The units for soil stiffness used in Figure 14 are kips per square foot per foot displacement, or kips per cubic foot, which is referred to as the soil constant, k. Typical values of k for flexible retaining structures in sand range between 5 and 40 kips per cubic foot, with 16 kips per cubic foot for a medium sand [13]. As shown by Figure 14, the soil stiffness values obtained by the method described herein compare favorably with these values. Figure 14 indicates a nearly linear relationship between depth and soil stiffness, varying only at the elevation extremes, where perimeter effects would normally be expected. Support spring constants were calculated at each node by multiplying the appropriate tributary area by the spring constant corresponding to the node elevation.

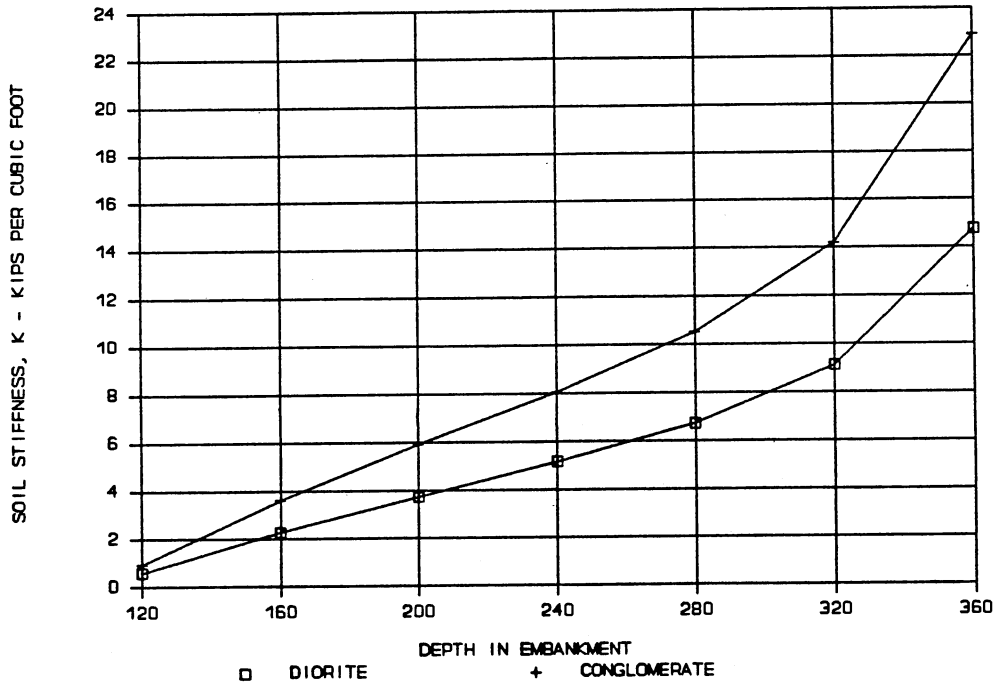

Figure 14. Soil Stiffness Vs Elevation

Perimeter Model

Mud Mountain Dam is constructed across a narrow canyon with steep rock walls more than 200 feet high on both sides (Figure 12). Perimeter effects under such conditions are a significant factor in the behavior of the wall-soil system. Maximum stresses in the wall will tend to occur due to the relatively high degree of fixity provided by the rock interface. These stresses will be strongly influenced by the ability of the rock to support rotation and translation, and increase as a function of the rock stiffness. Geologic exploration indicates the rock quality is highly variable throughout the interface area. The modulus of elasticity is estimated to range between 200,000 and 2,000,000 psi, with a median value of approximately 500,000 psi. The results of two plate

bearing tests which were performed on the rock abutments [9] indicate a deformational resistance of up to approximately 400 kips per cubic inch.

The behavior of the rock interface is accounted for in the grid structure model as a system of rotational and translational support springs at the perimeter nodes. Spring constants were developed by means of a beam on the elastic foundation model of the wall-rock interface, analyzed using the computer program CBEAMC [1]. The model consists of a 1-foot section of wall supported by a distributed linear spring for a distance of 15 feet, which corresponds to the minimum depth of key into rock required by the contract documents. Recognizing that it would be impractical to attempt to model the variations in rock stiffness present at the site, a singular spring constant of 4800 kips per inch per inch was used, which corresponds to the upper limit of the values of rock stiffness determined in the plate bearing tests. This value was selected to produce higher, hence more conservative, spring constants. Rotational and translational stiffnesses were determined by the application of a moment and force to one end of the model in separate load cases, and relating the displacements thus obtained to the applied loads.

The same beam on the elastic foundation model was also utilized to determine perimeter stiffness in the overburden above the rock. The overburden in the project area is a relatively stiff material and a correspondingly high modulus value of 0.417 kips per inch per inch was used as a distributed spring constant in the model. This equates to a soil k value of 60 kips per cubic foot or 0.035 kips per cubic inch.

Allowable Concrete Stresses

Flexural and shear stresses were determined from the computed

forces, based on section properties for individual grid members according to tributary area. These values were compared with allowable stress levels for flexure and shear. Allowable flexural tensile stress was assumed to be equal to 7.5 $\sqrt{f'_c}$, according to the ACI Code equation for the modulus of rupture. Allowable shear stress was assumed to be equal to 2 $\sqrt{f'_c}$, also according to the ACI Code.

Initial Results--Joint Continuity Throughout

The initial analysis was run assuming vertical and horizontal moment continuity throughout the structure. Results of this analysis indicate a high incidence of overstress, particularly along the rock interface, and generally increasing in magnitude with depth. Flexural overstressing was found to be more prevalent than shear overstressing, with virtually all members below pool level exceeding allowable stress. Stresses using the diorite shell parameters average approximately 30 percent greater than those using the stiffer conglomerate shell parameters. Maximum flexural stresses were found to be exceptionally high in some members, ranging to over 41 times allowable for the conglomerate shell and 50 times allowable for the diorite shell. Tables 1 and 2 (see Appendix) provide a summary showing the absolute values of the maximum bending moment and corresponding theoretical flexural tensile stress for each member in the grid model. The magnitude of overstressing evident in this summary indicates flexural cracking of the wall to be inevitable for the assumed conditions of load and support. The maximum shear stress was 13.2 times allowable for the conglomerate and 16.4 times allowable for the diorite. Flexural stresses in horizontal members were found to be influenced not only by depth but also by span, increasing signifi-

cantly in narrower portions of the model. Such trends were not as easily identified in the case of vertical grid members, which were generally not nearly as highly stressed. However, a notable concentration of higher stress levels was indicated in some of the vertical members in the upper center portion of the model. These members, located at or near the top of the input hydrostatic loads, are subject to only relatively small displacements. Bending stresses are therefore induced in these members as a result of the larger displacements of adjacent members at greater depths. This effect was confirmed by comparison of the deflected shape along the centerline of the grid structure model with that of the finite element model, as shown in Figures 15 and 16. This comparison reveals good correlation between the two models for nodal displacements below pool level, with much smaller displacements occurring above pool level in the grid structure model. This deflection geometry is consistent with the additional influence of the wall elements in the grid model in resisting deformation.

Results With Moments Released

Moment resistance at the vertical panel joints is expected to be influenced by a combination of two factors--joint width and bond strength. A reduced effective section to resist bending will occur due to deviation from exact alignment between adjacent panels, resulting in a reduced joint width. Such deviation is generally acknowledged to be unavoidable with this construction process, although it may be held to a minimum with careful execution of the excavation procedures. Maintenance of panel alignment is enforced by means of a requirement for a minimum joint width in the contract specifications. This requirement

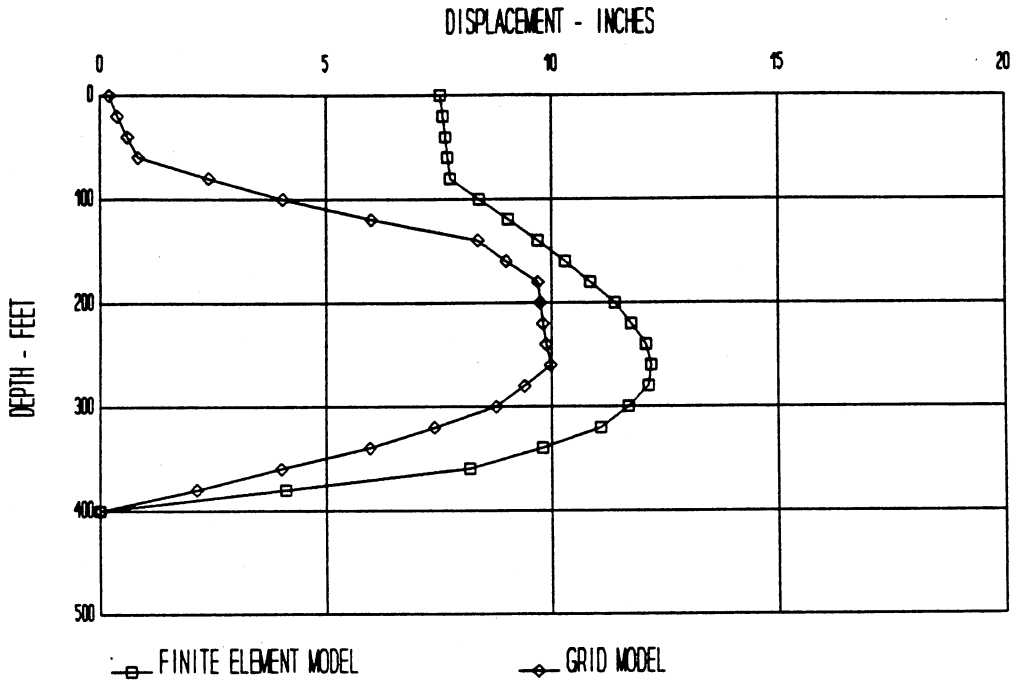

Figure 15. Wall Displacement Vs Depth--
Conglomerate Shell

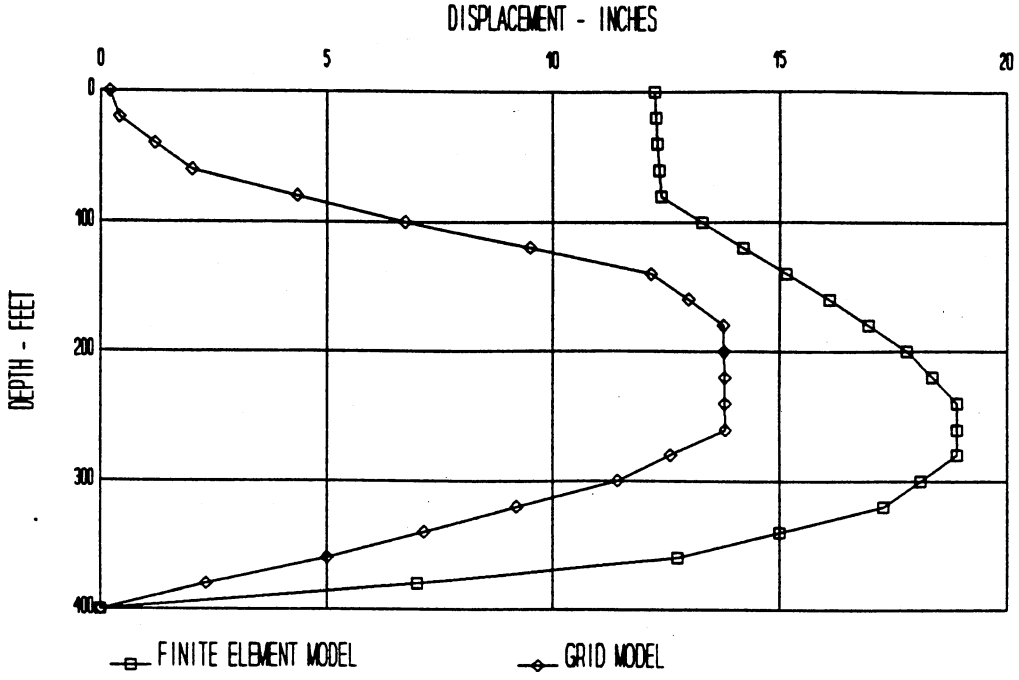

Figure 16. Wall Displacement Vs Depth--
Diorite Shell

was 24 inches in the case of the Mud Mountain installation, representing a 40 percent reduction in effective section depth at the joints, which corresponds to a 64 percent reduction in flexural strength.

Moment resistance at the joint is also affected by the tensile capacity of the concrete bond across the joint face. The texture of the excavated concrete surface produced by the panel installation process is expected to be conducive to the development of good bond strength. However, bond strength at the joint face may be detrimentally affected by inclusions of the bentonite slurry mixture, which can potentially be trapped by surface irregularities along the joint face. The net effect of these two factors on bond tensile strength is unknown, although it is unlikely that such bond will be equal in tensile capacity to continuous concrete. When this factor is considered with regard to the already significant strength reduction possible with a reduced effective section, it can be seen that cracking may occur at the joints under much lower force levels than would be required for continuous concrete.

In order to account for the presence of the panel joints in the wall, model behavior was re-evaluated after moment resistance about the vertical axis was released at the joints. Although increases in maximum displacement were generally on the order of 10 to 20 percent at various elevations due to this modification, the most pronounced effect was on the overall deformed shape of the model. By eliminating the deformational resistance provided by the wall stiffness spanning horizontally across the canyon, the model is allowed to assume a deflected shape more closely reflecting an equilibrium position between the hydrostatic driving forces and soil resistive forces. Maximum relative increases in displacement therefore occur close to the wall perimeter for this case,

where the flexural stiffness of the wall previously had the maximum effect in limiting movement. This effect is visible in Figures 17 and 18, which compare plan sections of the deflected position of the wall before and after moments are released. Member force results were also evaluated for this case and are summarized in Tables 3 through 6 (see Appendix). Bending forces in vertical grid members were found to be generally higher than in the fixed end cases, although exceptions can be found. Shear was also summarized for this analysis case and can be seen to exceed allowable values, but typically not to the extent of flexural overstress. Horizontal grid elements do not carry either shear or bending moment for this case, as would be expected with the given releases.

Grid Results Verification

Verification of the grid structure results was accomplished by means of the continuous beam analysis program CBEAMC [1]. The CBEAMC model consisted of a beam 75 feet in length corresponding to the horizontal grid elements at elevation 920, with matching element area, moment of inertia, and modulus of elasticity. As in the grid structure model, concentrated linear spring supports were located every 15 feet and the hydrostatic load was also applied at these locations. The support spring constants used for this comparison were the conglomerate rockfill shell values.

The results of the CBEAMC analysis correlate well with the CGRID results. Comparisons of displacements and bending moment are presented in Figures 19 and 20. As can be seen in Figure 19, the grid model deflection is unsymmetrical and slightly less than that of the one-dimensional beam model. This is as expected due to the influence of

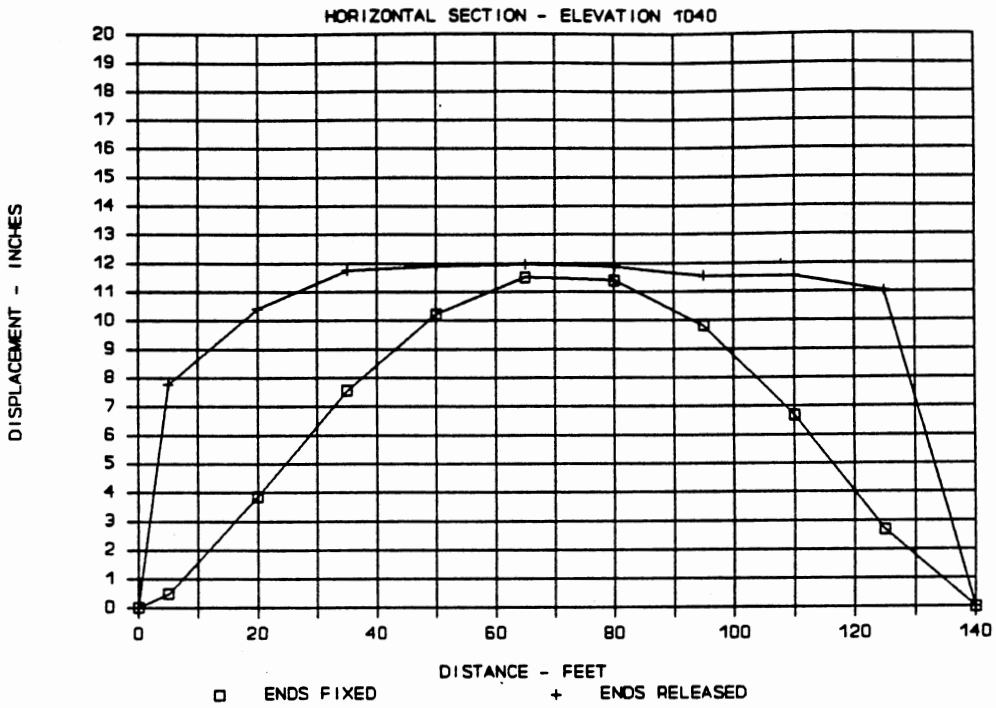

Figure 17. Horizontal Section--
Conglomerate Shell

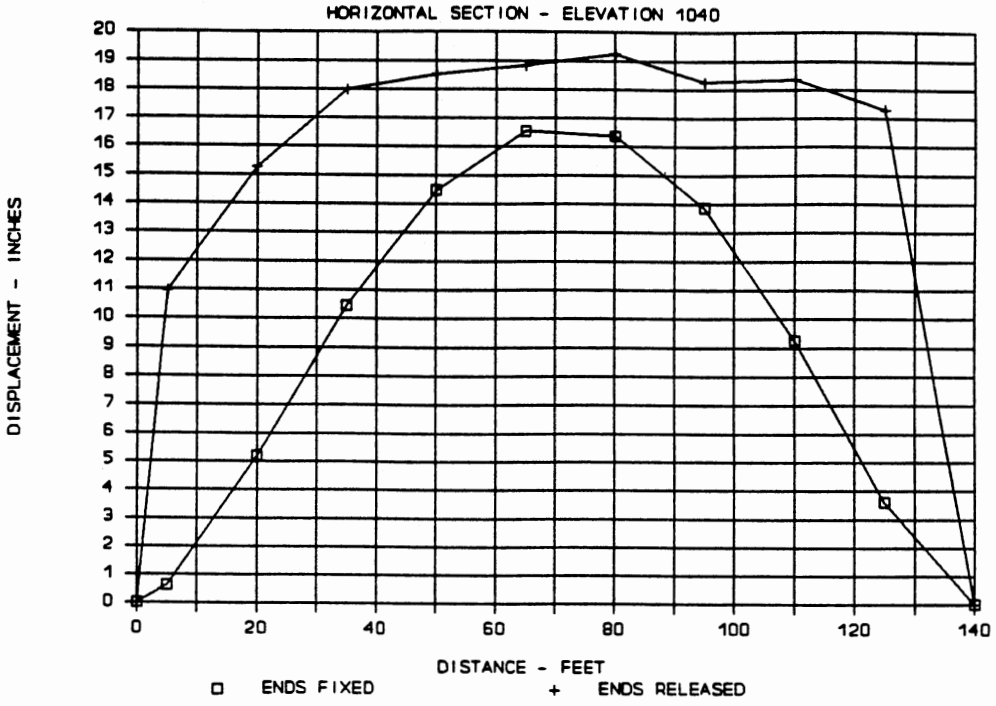

Figure 18. Horizontal Shell--
Diorite Shell

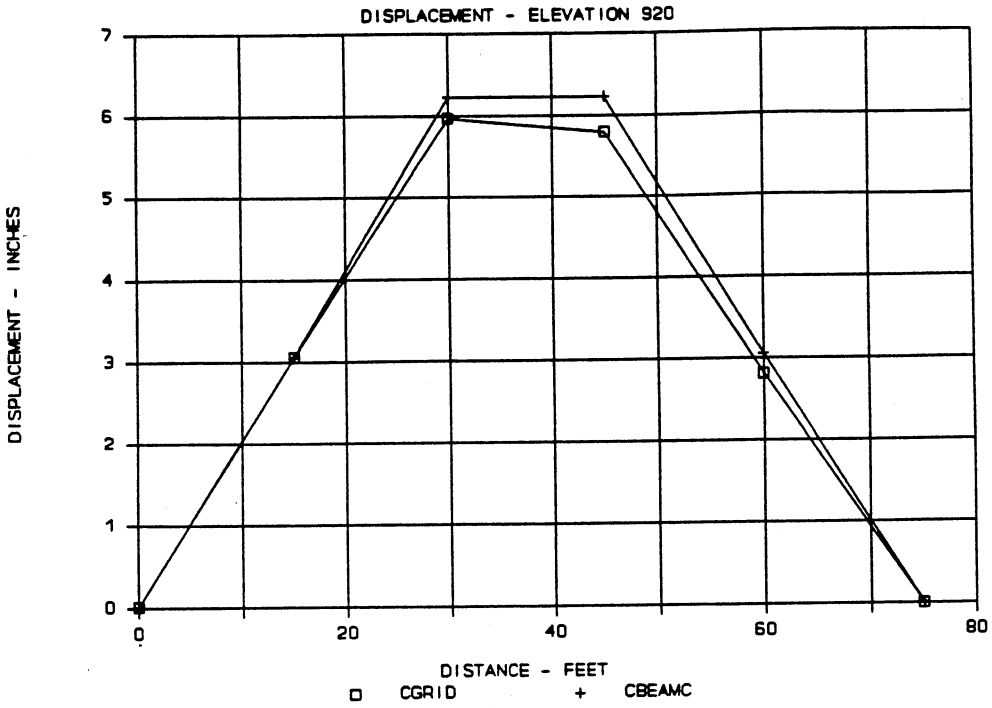

Figure 19. CGRID Results Verification--Displacement

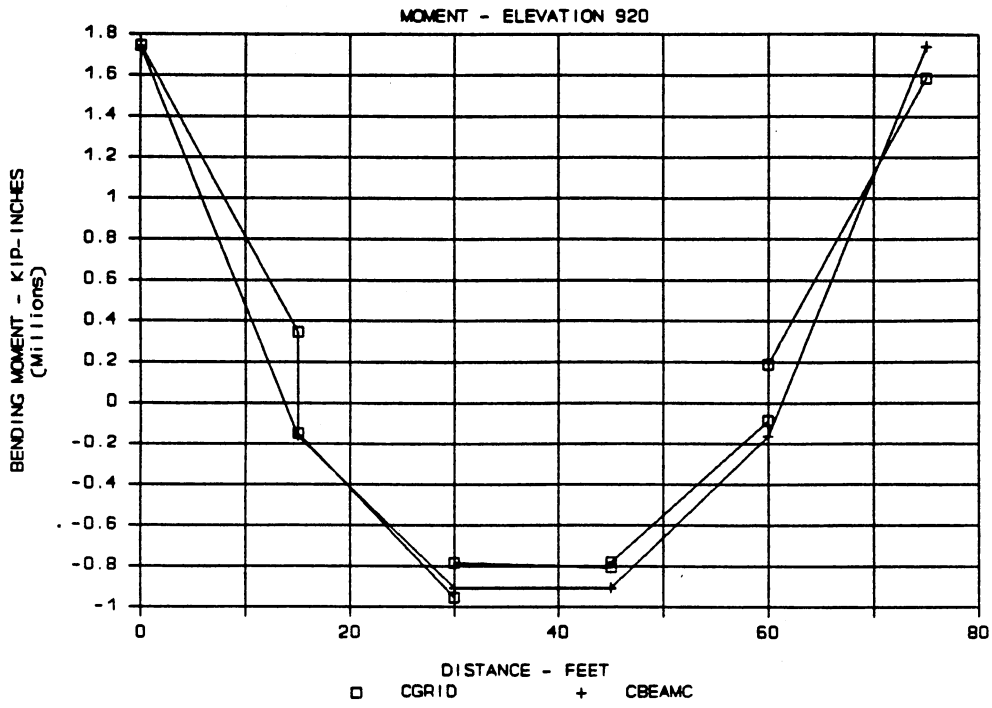

Figure 20. CGRID Results Verification--Moment

two-way wall action and adjacent perimeter geometry. Shear and bending moment were found to be similarly comparable, the CBEAMC results indicating a symmetrical condition not representative of the more complex grid model.

CHAPTER V

SUMMARY

A possible method for the analysis of diaphragm cutoff walls in embankment dams has been described and demonstrated. However, the application of this procedure in the subject investigation required the use of a number of assumptions relating to embankment response characteristics and loading. Although consideration has been given to the development of reasonable values with regard to these parameters, the applicable site data were insufficient to preclude the use of such assumptions. It is therefore necessary in interpreting the quantitative data thus obtained to be cognizant of the collective degree of uncertainty inherent under these circumstances.

By far the highest degree of uncertainty with regard to this investigation pertáins to the assumed loading condition. It is unlikely that the seepage cutoff wall at Mud Mountain Dam will ever be subjected to the full hydrostatic pressure differential of nearly 300 feet used in this analysis, since this would require 100 percent efficiency of the diaphragm wall as well as complete cessation of water migration through the perimeter rock. In the event of the occurrence of such a load, the findings indicate that it would probably not be present for any extended period of time, due to the associated overstressing and crack formation. By providing seepage paths through the wall, crack formation would relieve hydrostatic pressures in affected areas. Loading conditions

under which cracking is expected to occur are therefore difficult to predict because of the complex relationship between crack formation and load distribution. In actuality, seepage around the wall through the moderately faulted rock abutments should provide pressure relief by permitting the formation of a counteracting hydrostatic pressure distribution on the downstream face of the wall. Additional pressure relief may occur due to seepage through joints in the wall, although such seepage may be undesirable if it becomes excessive. The loading condition assumed for this investigation does not account for either of these sources of pressure equalization and therefore may be seen as quite conservative.

The high degree of overstressing revealed by this exercise indicates that crack formation in the wall may occur at an appreciably lower pressure differential than that utilized for this analysis, disallowing the effects of seepage. Due to the previously described relationship between crack formation and pressure distribution, displacements of the magnitude indicated by the analysis are not expected to occur. Displacements would presumably be limited to the point at which seepage resulting from crack formation serves to relieve the differential pressure at the affected area. Considering the limited moment capacity of the vertical panel joints, this point would potentially occur after only relatively minor displacements have taken place, possibly as little as 1 or 2 inches at the canyon centerline.

In spite of these uncertainties which stem from the basic nature of the problem, much can be learned from the results of this investigation. Cracking of the wall, if it occurs, will most likely be along the rock interface due to the major discontinuity in support stiffness between

the soil and rock media. The high ratio of horizontal member stresses to vertical member stresses indicates that cracking would be expected to initially take place along the vertical panel joints at the rock interface at lower pool levels. With increasing pool elevation, cracking would also be expected along horizontal portions of the rock interface at the deepest portion of the wall. Reduction of flexural stresses would require a joint accommodating rotation in these areas, and it is uncertain that a design for such could be achieved which prevents seepage.

The findings of this investigation should not be construed as predicting unsatisfactory performance for the seepage cutoff wall at Mud Mountain Dam. The design of the installation is based largely on similar installations at other sites, experience with which has been acceptable. A monitoring program consisting of a system of piezometers, survey monuments, and inclinometers has been included in the installation, which will provide useful information pertaining to loading conditions and deformation response of the wall. The investigation method described provides a means of assessing these data when they become available, making possible a better understanding of the behavior of these structures.

REFERENCES

[1] Dawkins, W. P. User's Guide: Computer Program for Analysis of Beam-Column Structures With Nonlinear Supports (CBEAMC). Vicksburg, MS: U.S.A.E. Waterways Experiment Station, 1982.

[2] Adhya, K. "Stress and Deformation Analysis of the Diaphragm Wall." U.S. Bureau of Reclamation Technical Memorandum FO-230-5, Dec., 1986.

[3] Chugh, A. K. Deformation Analysis of a Diaphragm Wall. Washington, DC: U.S. Dept. of the Interior, Bureau of Reclamation, 1987.

[4] Dascal, O. "Structural Behaviour of the Manicouagan 3 Cutoff." Canadian Geotechnical Journal, Vol. 16 (1979), pp. 200-221.

[5] Dawkins, W. P. Program CGRID--Computer Program for Analysis of Planar Grid Structures. Vicksburg, MS: U.S.A.E. CASE Task Group on Building Systems, June, 1987.

[6] Duncan, J. M., F. H. Kulhawy, and H. B. Seed. Finite Element Analysis of Stresses and Movements in Embankments During Construction. Berkeley: College of Engineering, University of Califoria, Nov., 1969.

[7] Duncan, J. M., and C. Y. Chang. "Nonlinear Analysis of Stress and Strain in Soils." Journal of the Soil Mechanics and Foundations Div., ASCE, Vol. 96 (Sept., 1970), pp. 1629-1653.

[8] Duncan, J. M., P. Byrne, K. S. Wong, and P. Mabry. Strength, Stress-Strain and Bulk Modulus Parameters for Finite Element Analysis of Stresses and Movements in Soil Masses. Report No. UCB/GT/80-01. Berkeley: College of Engineering, University of California, Aug., 1980.

[9] Analysis of Design--Mud Mountain Dam. Seattle: U.S. Dept. of the Army, May, 1946.

[10] Bathe, K. J. ADINA, A Finite Element Program for Automatic Dynamic Incremental Nonlinear Analysis. Cambridge: MIT, Dec., 1978.

[11] GTICES Systems Laboratory. GTSTRUDL. Version 84.02. Atlanta: School of Civil Engineering, Georgia Institute of Technology, 1981.

[12] Wilson, E. L. SOLID SAP, A Static Analysis Program for Three-Dimensional Solid Structures. Report No. UCSESM 71-19. Berkeley: Structural Engineering Laboratory, University of California, 1971.

[13] Haliburton, T. A. Soil-Structure Interaction: Numerical Analysis of Beams and Beam-Columns. Stillwater: School of Civil Engineering, Oklahoma State University, 1979.

APPENDIX

ELEMENT STRESS SUMMARIES

TABLE 1

FLEXURE: DIORITE SHELL--PANEL JOINTS FIXED

MEMBER NUMBER	DEPTH h INCHES	WIDTH b FEET	SECTION MODULUS IN-3	BENDING MOMENT IN-KIPS	FLEXURAL STRESS KSI	ALLOWABLE FLEXURAL STRESS	FLEXURAL STRESS RATIO
1	32	40	81920	187	0.00	0.41	0.01
2	32	40	81920	2122	0.03	0.41	0.06
3	32	40	81920	8330	0.10	0.41	0.25
4	32	40	81920	24140	0.29	0.41	0.72
5	32	40	81920	7937	0.10	0.41	0.24
6	32	40	81920	13150	0.16	0.41	0.39
7	32	40	81920	13960	0.17	0.41	0.42
8	32	40	81920	18590	0.23	0.41	0.55
9	32	40	81920	8048	0.10	0.41	0.24
10	32	40	81920	2715	0.03	0.41	0.08
11	32	40	81920	1048	0.01	0.41	0.03
12	32	85	174080	1556	0.01	0.41	0.02
13	32	75	153600	5116	0.03	0.41	0.08
14	32	60	122880	10410	0.08	0.41	0.21
15	32	45	92160	37070	0.40	0.41	0.98
16	32	45	92160	43160	0.47	0.41	1.14
17	32	60	122880	63810	0.52	0.41	1.27
18	32	60	122880	36930	0.30	0.41	0.73
19	32	60	122880	12920	0.11	0.41	0.26
20	32	60	122880	5094	0.04	0.41	0.10
21	32	60	122880	1691	0.01	0.41	0.03
22	32	40	81920	2715	0.03	0.41	0.08
23	32	40	81920	13960	0.17	0.41	0.42
24	32	40	81920	17480	0.21	0.41	0.52
25	32	40	81920	17560	0.21	0.41	0.52
26	32	40	81920	22200	0.27	0.41	0.66
27	32	40	81920	10060	0.12	0.41	0.30
28	32	40	81920	15080	0.18	0.41	0.45
29	32	40	81920	8722	0.11	0.41	0.26
30	32	40	81920	2011	0.02	0.41	0.06
31	32	60	122880	3255	0.03	0.41	0.06
32	32	60	122880	19040	0.15	0.41	0.38
33	32	45	92160	44760	0.49	0.41	1.18
34	32	45	92160	67040	0.73	0.41	1.77
35	32	60	122880	97320	0.79	0.41	1.93
36	32	60	122880	35460	0.29	0.41	0.70
37	32	60	122880	10180	0.08	0.41	0.20
38	32	60	122880	4192	0.03	0.41	0.08
39	32	40	81920	27800	0.34	0.41	0.83
40	32	40	81920	64440	0.79	0.41	1.92
41	32	40	81920	8536	0.10	0.41	0.25
42	32	40	81920	33950	0.41	0.41	1.01
43	32	40	81920	45520	0.56	0.41	1.36
44	32	40	81920	45650	0.56	0.41	1.36
45	32	40	81920	47040	0.57	0.41	1.40
46	32	40	81920	22530	0.28	0.41	0.67
47	32	40	81920	33110	0.40	0.41	0.99
48	32	40	81920	11970	0.15	0.41	0.36
49	32	30	61440	40840	0.66	0.41	1.62
50	32	30	61440	68940	1.12	0.41	2.74
51	32	30	61440	116400	1.89	0.41	4.62
52	32	30	61440	151900	2.47	0.41	6.03
53	32	30	61440	147700	2.40	0.41	5.86
54	32	30	61440	147400	2.40	0.41	5.85
55	32	30	61440	148500	2.42	0.41	5.90
56	32	45	92160	209600	2.27	0.41	5.55
57	32	45	92160	30620	0.33	0.41	0.81
58	40	40	128000	416300	3.25	0.41	7.93

TABLE 1 (CONTINUED)

MEMBER NUMBER	DEPTH h INCHES	WIDTH b FEET	SECTION MODULUS IN-3	BENDING MOMENT IN-KIPS	FLEXURAL STRESS KSI	ALLOWABLE FLEXURAL STRESS	FLEXURAL STRESS RATIO
59	40	40	128000	194500	1.52	0.41	3.71
60	40	40	128000	93860	0.73	0.41	1.79
61	40	40	128000	162600	1.27	0.41	3.10
62	40	40	128000	196300	1.53	0.41	3.74
63	40	40	128000	197600	1.54	0.41	3.77
64	40	40	128000	113500	0.89	0.41	2.16
65	40	40	128000	60850	0.48	0.41	1.16
66	40	40	128000	161700	1.26	0.41	3.08
67	40	40	128000	81900	0.64	0.41	1.56
68	40	30	96000	291700	3.04	0.41	7.41
69	40	23	72000	130200	1.81	0.41	4.41
70	40	15	48000	57570	1.20	0.41	2.93
71	40	23	72000	113200	1.57	0.41	3.83
72	40	30	96000	147200	1.53	0.41	3.74
73	40	30	96000	110100	1.15	0.41	2.80
74	40	23	72000	127600	1.77	0.41	4.32
75	40	15	48000	160200	3.34	0.41	8.14
76	40	23	72000	399600	5.55	0.41	13.54
77	40	40	128000	927600	7.25	0.41	17.68
78	40	40	128000	126200	0.99	0.41	2.40
79	40	40	128000	238900	1.87	0.41	4.55
80	40	40	128000	325500	2.54	0.41	6.20
81	40	40	128000	370200	2.89	0.41	7.05
82	40	40	128000	360000	2.81	0.41	6.86
83	40	40	128000	105400	0.82	0.41	2.01
84	40	40	128000	1232000	9.63	0.41	23.48
85	40	15	48000	264200	5.50	0.41	13.42
86	40	15	48000	162900	3.39	0.41	8.28
87	40	23	72000	96340	1.34	0.41	3.26
88	40	30	96000	94330	0.98	0.41	2.40
89	40	30	96000	18370	0.19	0.41	0.47
90	40	23	72000	193600	2.69	0.41	6.56
91	40	23	72000	123500	1.72	0.41	4.18
92	40	40	128000	1784000	13.94	0.41	33.99
93	40	40	128000	1219000	9.52	0.41	23.23
94	40	40	128000	435000	3.40	0.41	8.29
95	40	40	128000	480600	3.75	0.41	9.16
96	40	40	128000	548700	4.29	0.41	10.46
97	40	40	128000	543100	4.24	0.41	10.35
98	40	40	128000	595700	4.65	0.41	11.35
99	40	40	128000	615400	4.81	0.41	11.73
100	40	40	128000	400600	3.13	0.41	7.63
101	40	40	128000	1788000	13.97	0.41	34.07
102	40	15	48000	23680	0.49	0.41	1.20
103	40	15	48000	30140	0.63	0.41	1.53
104	40	15	48000	45530	0.95	0.41	2.31
105	40	15	48000	72220	1.50	0.41	3.67
106	40	15	48000	82540	1.72	0.41	4.19
107	40	15	48000	85880	1.79	0.41	4.36
108	40	15	48000	71320	1.49	0.41	3.62
109	40	15	48000	52000	1.08	0.41	2.64
110	40	15	48000	45700	0.95	0.41	2.32
111	40	15	48000	118	0.00	0.41	0.01
112	40	40	128000	1184000	9.25	0.41	22.56
113	40	40	128000	617800	4.83	0.41	11.77
114	40	40	128000	382200	2.99	0.41	7.28
115	40	40	128000	473700	3.70	0.41	9.03
116	40	40	128000	596900	4.66	0.41	11.37
117	40	40	128000	691100	5.40	0.41	13.17
118	40	40	128000	720800	5.63	0.41	13.73
119	40	40	128000	465000	3.63	0.41	8.86

TABLE 1 (CONTINUED)

MEMBER NUMBER	DEPTH h INCHES	WIDTH b FEET	SECTION MODULUS IN-3	BENDING MOMENT IN-KIPS	FLEXURAL STRESS KSI	ALLOWABLE FLEXURAL STRESS	FLEXURAL STRESS RATIO
120	40	40	128000	1934000	15.11	0.41	36.85
121	40	15	48000	488800	10.18	0.41	24.84
122	40	15	48000	275300	5.74	0.41	13.99
123	40	15	48000	252100	5.25	0.41	12.81
124	40	15	48000	188500	3.93	0.41	9.58
125	40	15	48000	76440	1.59	0.41	3.88
126	40	15	48000	66760	1.39	0.41	3.39
127	40	15	48000	74310	1.55	0.41	3.78
128	40	15	48000	44650	0.93	0.41	2.27
129	40	40	128000	620200	4.85	0.41	11.82
130	40	40	128000	1121000	8.76	0.41	21.36
131	40	40	128000	789300	6.17	0.41	15.04
132	40	40	128000	939000	7.34	0.41	17.89
133	40	40	128000	947700	7.40	0.41	18.06
134	40	40	128000	748900	5.85	0.41	14.27
135	40	40	128000	2037000	15.91	0.41	38.81
136	40	15	48000	1029000	21.44	0.41	52.29
137	40	15	48000	286700	5.97	0.41	14.57
138	40	15	48000	236300	4.92	0.41	12.01
139	40	15	48000	74380	1.55	0.41	3.78
140	40	15	48000	31160	0.65	0.41	1.58
141	40	15	48000	55310	1.15	0.41	2.81
142	40	40	128000	2061000	16.10	0.41	39.27
143	40	40	128000	1165000	9.10	0.41	22.20
144	40	40	128000	979400	7.65	0.41	18.66
145	40	40	128000	937500	7.32	0.41	17.86
146	40	40	128000	1857000	14.51	0.41	35.38
147	40	15	48000	44740	0.93	0.41	2.27
148	40	15	48000	79940	1.67	0.41	4.06
149	40	15	48000	142700	2.97	0.41	7.25
150	40	15	48000	117700	2.45	0.41	5.98
151	40	30	96000	747000	7.78	0.41	18.98
152	40	30	96000	309400	3.22	0.41	7.86
153	40	30	96000	392700	4.09	0.41	9.98
154	40	30	96000	238500	2.48	0.41	6.06
155	40	30	96000	580300	6.04	0.41	14.74
156	40	15	48000	233000	4.85	0.41	11.84
157	40	15	48000	530200	11.05	0.41	26.94
158	40	15	48000	574400	11.97	0.41	29.19
159	40	15	48000	93280	1.94	0.41	4.74

TABLE 2

FLEXURE: CONGLOMERATE SHELL--PANEL JOINTS FIXED

MEMBER NUMBER	DEPTH h INCHES	WIDTH b FEET	SECTION MODULUS IN-3	BENDING MOMENT IN-KIPS	FLEXURAL STRESS KSI	ALLOWABLE FLEXURAL STRESS	FLEXURAL STRESS RATIO
1	32	40	81920	29	0.00	0.41	0.00
2	32	40	81920	1711	0.02	0.41	0.05
3	32	40	81920	3272	0.04	0.41	0.10
4	32	40	81920	13600	0.17	0.41	0.40
5	32	40	81920	4869	0.06	0.41	0.14
6	32	40	81920	5961	0.07	0.41	0.18
7	32	40	81920	8278	0.10	0.41	0.25
8	32	40	81920	10330	0.13	0.41	0.31
9	32	40	81920	4143	0.05	0.41	0.12
10	32	40	81920	1131	0.01	0.41	0.03
11	32	40	81920	571	0.01	0.41	0.02
12	32	85	174080	437	0.00	0.41	0.01
13	32	75	153600	2714	0.02	0.41	0.04
14	32	60	122880	9925	0.08	0.41	0.20
15	32	45	92160	33160	0.36	0.41	0.88
16	32	45	92160	38180	0.41	0.41	1.01
17	32	60	122880	56330	0.46	0.41	1.12
18	32	60	122880	36130	0.29	0.41	0.72
19	32	60	122880	13910	0.11	0.41	0.28
20	32	60	122880	2967	0.02	0.41	0.06
21	32	60	122880	584	0.00	0.41	0.01
22	32	40	81920	1885	0.02	0.41	0.06
23	32	40	81920	8637	0.11	0.41	0.26
24	32	40	81920	11800	0.14	0.41	0.35
25	32	40	81920	14170	0.17	0.41	0.42
26	32	40	81920	11190	0.14	0.41	0.33
27	32	40	81920	9583	0.12	0.41	0.29
28	32	40	81920	10350	0.13	0.41	0.31
29	32	40	81920	5994	0.07	0.41	0.18
30	32	40	81920	1107	0.01	0.41	0.03
31	32	60	122880	1560	0.01	0.41	0.03
32	32	60	122880	17500	0.14	0.41	0.35
33	32	45	92160	39740	0.43	0.41	1.05
34	32	45	92160	51700	0.56	0.41	1.37
35	32	60	122880	74620	0.61	0.41	1.48
36	32	60	122880	37530	0.31	0.41	0.74
37	32	60	122880	16410	0.13	0.41	0.33
38	32	60	122880	4983	0.04	0.41	0.10
39	32	40	81920	18900	0.23	0.41	0.56
40	32	40	81920	43370	0.53	0.41	1.29
41	32	40	81920	4342	0.05	0.41	0.13
42	32	40	81920	29910	0.37	0.41	0.89
43	32	40	81920	19910	0.24	0.41	0.59
44	32	40	81920	24200	0.30	0.41	0.72
45	32	40	81920	32120	0.39	0.41	0.96
46	32	40	81920	17360	0.21	0.41	0.52
47	32	40	81920	21080	0.26	0.41	0.63
48	32	40	81920	9915	0.12	0.41	0.30
49	32	30	61440	30070	0.49	0.41	1.19
50	32	30	61440	65730	1.07	0.41	2.61
51	32	30	61440	100500	1.64	0.41	3.99
52	32	30	61440	120900	1.97	0.41	4.80
53	32	30	61440	113400	1.85	0.41	4.50
54	32	30	61440	118800	1.93	0.41	4.72
55	32	30	61440	125500	2.04	0.41	4.98
56	32	45	92160	186300	2.02	0.41	4.93
57	32	45	92160	34030	0.37	0.41	0.90
58	40	40	128000	345900	2.70	0.41	6.59

TABLE 2 (CONTINUED)

MEMBER NUMBER	DEPTH h INCHES	WIDTH b FEET	SECTION MODULUS IN-3	BENDING MOMENT IN-KIPS	FLEXURAL STRESS KSI	ALLOWABLE FLEXURAL STRESS	FLEXURAL STRESS RATIO
59	40	40	128000	113700	0.89	0.41	2.17
60	40	40	128000	78670	0.61	0.41	1.50
61	40	40	128000	130500	1.02	0.41	2.49
62	40	40	128000	132600	1.04	0.41	2.53
63	40	40	128000	111400	0.87	0.41	2.12
64	40	40	128000	62170	0.49	0.41	1.18
65	40	40	128000	18840	0.15	0.41	0.36
66	40	40	128000	98680	0.77	0.41	1.88
67	40	40	128000	64850	0.51	0.41	1.24
68	40	30	96000	236800	2.47	0.41	6.02
69	40	23	72000	99180	1.38	0.41	3.36
70	40	15	48000	48490	1.01	0.41	2.46
71	40	23	72000	88450	1.23	0.41	3.00
72	40	30	96000	106600	1.11	0.41	2.71
73	40	30	96000	86900	0.91	0.41	2.21
74	40	23	72000	96140	1.34	0.41	3.26
75	40	15	48000	127300	2.65	0.41	6.47
76	40	23	72000	323700	4.50	0.41	10.97
77	40	40	128000	728800	5.69	0.41	13.89
78	40	40	128000	123300	0.96	0.41	2.35
79	40	40	128000	173300	1.35	0.41	3.30
80	40	40	128000	215600	1.68	0.41	4.11
81	40	40	128000	227100	1.77	0.41	4.33
82	40	40	128000	240900	1.88	0.41	4.59
83	40	40	128000	292600	2.29	0.41	5.58
84	40	40	128000	980100	7.66	0.41	18.68
85	40	15	48000	203200	4.23	0.41	10.33
86	40	15	48000	121700	2.54	0.41	6.18
87	40	23	72000	68370	0.95	0.41	2.32
88	40	30	96000	58960	0.61	0.41	1.50
89	40	30	96000	8273	0.09	0.41	0.21
90	40	23	72000	148000	2.06	0.41	5.01
91	40	23	72000	96650	1.34	0.41	3.27
92	40	40	128000	1374000	10.73	0.41	26.18
93	40	40	128000	899200	7.03	0.41	17.13
94	40	40	128000	350400	2.74	0.41	6.68
95	40	40	128000	327300	2.56	0.41	6.24
96	40	40	128000	355000	2.77	0.41	6.76
97	40	40	128000	337700	2.64	0.41	6.43
98	40	40	128000	375600	2.93	0.41	7.16
99	40	40	128000	431700	3.37	0.41	8.23
100	40	40	128000	268900	2.10	0.41	5.12
101	40	40	128000	1358000	10.61	0.41	25.88
102	40	15	48000	18860	0.39	0.41	0.96
103	40	15	48000	25800	0.54	0.41	1.31
104	40	15	48000	41100	0.86	0.41	2.09
105	40	15	48000	59670	1.24	0.41	3.03
106	40	15	48000	62510	1.30	0.41	3.18
107	40	15	48000	59830	1.25	0.41	3.04
108	40	15	48000	47850	1.00	0.41	2.43
109	40	15	48000	34720	0.72	0.41	1.76
110	40	15	48000	34620	0.72	0.41	1.76
111	40	15	48000	106	0.00	0.41	0.01
112	40	40	128000	94700	0.74	0.41	1.80
113	40	40	128000	418100	3.27	0.41	7.97
114	40	40	128000	278900	2.18	0.41	5.31
115	40	40	128000	297200	2.32	0.41	5.66
116	40	40	128000	380100	2.97	0.41	7.24
117	40	40	128000	453900	3.55	0.41	8.65
118	40	40	128000	507200	3.96	0.41	9.66
119	40	40	128000	382600	2.99	0.41	7.29

TABLE 2 (CONTINUED)

MEMBER NUMBER	DEPTH h INCHES	WIDTH b FEET	SECTION MODULUS IN-3	BENDING MOMENT IN-KIPS	FLEXURAL STRESS KSI	ALLOWABLE FLEXURAL STRESS	FLEXURAL STRESS RATIO
120	40	40	128000	1499000	11.71	0.41	28.56
121	40	15	48000	386100	8.04	0.41	19.62
122	40	15	48000	210700	4.39	0.41	10.71
123	40	15	48000	184900	3.85	0.41	9.40
124	40	15	48000	124900	2.60	0.41	6.35
125	40	15	48000	38870	0.81	0.41	1.98
126	40	15	48000	62600	1.30	0.41	3.18
127	40	15	48000	59420	1.24	0.41	3.02
128	40	15	48000	32030	0.67	0.41	1.63
129	40	40	128000	456200	3.56	0.41	8.69
130	40	40	128000	858700	6.71	0.41	16.36
131	40	40	128000	570600	4.46	0.41	10.87
132	40	40	128000	687900	5.37	0.41	13.11
133	40	40	128000	706600	5.52	0.41	13.46
134	40	40	128000	600300	4.69	0.41	11.44
135	40	40	128000	1644000	12.84	0.41	31.33
136	40	15	48000	811500	16.91	0.41	41.23
137	40	15	48000	228300	4.76	0.41	11.60
138	40	15	48000	175300	3.65	0.41	8.91
139	40	15	48000	40590	0.85	0.41	2.06
140	40	15	48000	37880	0.79	0.41	1.92
141	40	15	48000	48130	1.00	0.41	2.45
142	40	40	128000	1746000	13.64	0.41	33.27
143	40	40	128000	952900	7.44	0.41	18.16
144	40	40	128000	804600	6.29	0.41	15.33
145	40	40	128000	779500	6.09	0.41	14.85
146	40	40	128000	1588000	12.41	0.41	30.26
147	40	15	48000	48890	1.02	0.41	2.48
148	40	15	48000	62680	1.31	0.41	3.18
149	40	15	48000	117900	2.46	0.41	5.99
150	40	15	48000	104300	2.17	0.41	5.30
151	40	30	96000	698500	7.28	0.41	17.75
152	40	30	96000	281400	2.93	0.41	7.15
153	40	30	96000	353100	3.68	0.41	8.97
154	40	30	96000	221200	2.30	0.41	5.62
155	40	30	96000	534900	5.57	0.41	13.59
156	40	15	48000	218500	4.55	0.41	11.10
157	40	15	48000	490000	10.21	0.41	24.90
158	40	15	48000	529200	11.03	0.41	26.89
159	40	15	48000	87350	1.82	0.41	4.44

TABLE 3

FLEXURE: DIORITE SHELL--PANEL JOINTS RELEASED

MEMBER NUMBER	DEPTH h INCHES	WIDTH b FEET	SECTION MODULUS IN-3	BENDING MOMENT IN-KIPS	FLEXURAL STRESS KSI	ALLOWABLE FLEXURAL STRESS	FLEXURAL STRESS RATIO
1	32	40	81920	0	0.00	0.41	0.00
2	32	40	81920	0	0.00	0.41	0.00
3	32	40	81920	0	0.00	0.41	0.00
4	32	40	81920	0	0.00	0.41	0.00
5	32	40	81920	0	0.00	0.41	0.00
6	32	40	81920	0	0.00	0.41	0.00
7	32	40	81920	0	0.00	0.41	0.00
8	32	40	81920	0	0.00	0.41	0.00
9	32	40	81920	0	0.00	0.41	0.00
10	32	40	81920	0	0.00	0.41	0.00
11	32	40	81920	0	0.00	0.41	0.00
12	32	85	174080	534	0.00	0.41	0.01
13	32	75	153600	6209	0.04	0.41	0.10
14	32	60	122880	21800	0.18	0.41	0.43
15	32	45	92160	39250	0.43	0.41	1.04
16	32	45	92160	55880	0.61	0.41	1.48
17	32	60	122880	70900	0.58	0.41	1.41
18	32	60	122880	41040	0.33	0.41	0.81
19	32	60	122880	15630	0.13	0.41	0.31
20	32	60	122880	5100	0.04	0.41	0.10
21	32	60	122880	1087	0.01	0.41	0.02
22	32	40	81920	0	0.00	0.41	0.00
23	32	40	81920	0	0.00	0.41	0.00
24	32	40	81920	0	0.00	0.41	0.00
25	32	40	81920	0	0.00	0.41	0.00
26	32	40	81920	0	0.00	0.41	0.00
27	32	40	81920	0	0.00	0.41	0.00
28	32	40	81920	0	0.00	0.41	0.00
29	32	40	81920	0	0.00	0.41	0.00
30	32	40	81920	0	0.00	0.41	0.00
31	32	60	122880	10690	0.09	0.41	0.21
32	32	60	122880	36370	0.30	0.41	0.72
33	32	45	92160	82060	0.89	0.41	2.17
34	32	45	92160	70030	0.76	0.41	1.85
35	32	60	122880	96040	0.78	0.41	1.91
36	32	60	122880	41420	0.34	0.41	0.82
37	32	60	122880	22180	0.18	0.41	0.44
38	32	60	122880	11620	0.09	0.41	0.23
39	32	40	81920	0	0.00	0.41	0.00
40	32	40	81920	0	0.00	0.41	0.00
41	32	40	81920	0	0.00	0.41	0.00
42	32	40	81920	0	0.00	0.41	0.00
43	32	40	81920	0	0.00	0.41	0.00
44	32	40	81920	0	0.00	0.41	0.00
45	32	40	81920	0	0.00	0.41	0.00
46	32	40	81920	0	0.00	0.41	0.00
47	32	40	81920	0	0.00	0.41	0.00
48	32	40	81920	0	0.00	0.41	0.00
49	32	30	61440	42620	0.69	0.41	1.69
50	32	30	61440	85190	1.39	0.41	3.38
51	32	30	61440	159900	2.60	0.41	6.35
52	32	30	61440	119200	1.94	0.41	4.73
53	32	30	61440	108800	1.77	0.41	4.32
54	32	30	61440	120700	1.96	0.41	4.79
55	32	30	61440	160100	2.61	0.41	6.36
56	32	45	92160	160500	1.74	0.41	4.25
57	32	45	92160	24960	0.27	0.41	0.66
58	40	40	128000	0	0.00	0.41	0.00

TABLE 3 (CONTINUED)

MEMBER NUMBER	DEPTH h INCHES	WIDTH b FEET	SECTION MODULUS IN-3	BENDING MOMENT IN-KIPS	FLEXURAL STRESS KSI	ALLOWABLE FLEXURAL STRESS	FLEXURAL STRESS RATIO
59	40	40	128000	0	0.00	0.41	0.00
60	40	40	128000	0	0.00	0.41	0.00
61	40	40	128000	0	0.00	0.41	0.00
62	40	40	128000	0	0.00	0.41	0.00
63	40	40	128000	0	0.00	0.41	0.00
64	40	40	128000	0	0.00	0.41	0.00
65	40	40	128000	0	0.00	0.41	0.00
66	40	40	128000	0	0.00	0.41	0.00
67	40	40	128000	0	0.00	0.41	0.00
68	40	30	96000	396800	4.13	0.41	10.08
69	40	23	72000	126700	1.76	0.41	4.29
70	40	15	48000	38640	0.81	0.41	1.96
71	40	23	72000	117800	1.64	0.41	3.99
72	40	30	96000	96740	1.01	0.41	2.46
73	40	30	96000	114800	1.20	0.41	2.92
74	40	23	72000	175000	2.43	0.41	5.93
75	40	15	48000	127300	2.65	0.41	6.47
76	40	23	72000	404400	5.62	0.41	13.70
77	40	40	128000	0	0.00	0.41	0.00
78	40	40	128000	0	0.00	0.41	0.00
79	40	40	128000	0	0.00	0.41	0.00
80	40	40	128000	0	0.00	0.41	0.00
81	40	40	128000	0	0.00	0.41	0.00
82	40	40	128000	0	0.00	0.41	0.00
83	40	40	128000	0	0.00	0.41	0.00
84	40	40	128000	0	0.00	0.41	0.00
85	40	15	48000	130700	2.72	0.41	6.64
86	40	15	48000	59870	1.25	0.41	3.04
87	40	23	72000	159000	2.21	0.41	5.39
88	40	30	96000	100500	1.05	0.41	2.55
89	40	30	96000	55400	0.58	0.41	1.41
90	40	23	72000	103500	1.44	0.41	3.51
91	40	23	72000	431400	5.99	0.41	14.61
92	40	40	128000	0	0.00	0.41	0.00
93	40	40	128000	0	0.00	0.41	0.00
94	40	40	128000	0	0.00	0.41	0.00
95	40	40	128000	0	0.00	0.41	0.00
96	40	40	128000	0	0.00	0.41	0.00
97	40	40	128000	0	0.00	0.41	0.00
98	40	40	128000	0	0.00	0.41	0.00
99	40	40	128000	0	0.00	0.41	0.00
100	40	40	128000	0	0.00	0.41	0.00
101	40	40	128000	0	0.00	0.41	0.00
102	40	15	48000	380400	7.93	0.41	19.33
103	40	15	48000	234600	4.89	0.41	11.92
104	40	15	48000	169800	3.54	0.41	8.63
105	40	15	48000	99450	2.07	0.41	5.05
106	40	15	48000	134600	2.80	0.41	6.84
107	40	15	48000	85490	1.78	0.41	4.34
108	40	15	48000	48170	1.00	0.41	2.45
109	40	15	48000	16640	0.35	0.41	0.85
110	40	15	48000	68210	1.42	0.41	3.47
111	40	15	48000	69620	1.45	0.41	3.54
112	40	40	128000	0	0.00	0.41	0.00
113	40	40	128000	0	0.00	0.41	0.00
114	40	40	128000	0	0.00	0.41	0.00
115	40	40	128000	0	0.00	0.41	0.00
116	40	40	128000	0	0.00	0.41	0.00
117	40	40	128000	0	0.00	0.41	0.00
118	40	40	128000	0	0.00	0.41	0.00
119	40	40	128000	0	0.00	0.41	0.00

TABLE 3 (CONTINUED)

MEMBER NUMBER	DEPTH h INCHES	WIDTH b FEET	SECTION MODULUS IN-3	BENDING MOMENT IN-KIPS	FLEXURAL STRESS KSI	ALLOWABLE FLEXURAL STRESS	FLEXURAL STRESS RATIO
120	40	40	128000	0	0.00	0.41	0.00
121	40	15	48000	454500	9.47	0.41	23.09
122	40	15	48000	309300	6.44	0.41	15.72
123	40	15	48000	302800	6.31	0.41	15.39
124	40	15	48000	112700	2.35	0.41	5.73
125	40	15	48000	182700	3.81	0.41	9.28
126	40	15	48000	101900	2.12	0.41	5.18
127	40	15	48000	57650	1.20	0.41	2.93
128	40	15	48000	51070	1.06	0.41	2.60
129	40	40	128000	0	0.00	0.41	0.00
130	40	40	128000	0	0.00	0.41	0.00
131	40	40	128000	0	0.00	0.41	0.00
132	40	40	128000	0	0.00	0.41	0.00
133	40	40	128000	0	0.00	0.41	0.00
134	40	40	128000	0	0.00	0.41	0.00
135	40	40	128000	0	0.00	0.41	0.00
136	40	15	48000	314200	6.55	0.41	15.97
137	40	15	48000	504600	10.51	0.41	25.64
138	40	15	48000	212600	4.43	0.41	10.80
139	40	15	48000	182600	3.80	0.41	9.28
140	40	15	48000	152000	3.17	0.41	7.72
141	40	15	48000	104300	2.17	0.41	5.30
142	40	40	128000	0	0.00	0.41	0.00
143	40	40	128000	0	0.00	0.41	0.00
144	40	40	128000	0	0.00	0.41	0.00
145	40	40	128000	0	0.00	0.41	0.00
146	40	40	128000	0	0.00	0.41	0.00
147	40	15	48000	149900	3.12	0.41	7.62
148	40	15	48000	155400	3.24	0.41	7.90
149	40	15	48000	231800	4.83	0.41	11.78
150	40	15	48000	356400	7.43	0.41	18.11
151	40	30	96000	0	0.00	0.41	0.00
152	40	30	96000	0	0.00	0.41	0.00
153	40	30	96000	0	0.00	0.41	0.00
154	40	30	96000	0	0.00	0.41	0.00
155	40	30	96000	0	0.00	0.41	0.00
156	40	15	48000	488800	10.18	0.41	24.84
157	40	15	48000	423500	8.82	0.41	21.52
158	40	15	48000	409000	8.52	0.41	20.78
159	40	15	48000	332000	6.92	0.41	16.87

TABLE 4

SHEAR: DIORITE SHELL--PANEL JOINTS RELEASED

MEMBER NUMBER	DEPTH h INCHES	WIDTH b FEET	SHEAR AREA IN-2	SHEAR FORCE KIPS	SHEAR STRESS KSI	ALLOWABLE SHEAR STRESS	SHEAR STRESS RATIO
1	32	40	15360	0	0.00	0.11	0.00
2	32	40	15360	0	0.00	0.11	0.00
3	32	40	15360	0	0.00	0.11	0.00
4	32	40	15360	0	0.00	0.11	0.00
5	32	40	15360	0	0.00	0.11	0.00
6	32	40	15360	0	0.00	0.11	0.00
7	32	40	15360	0	0.00	0.11	0.00
8	32	40	15360	0	0.00	0.11	0.00
9	32	40	15360	0	0.00	0.11	0.00
10	32	40	15360	0	0.00	0.11	0.00
11	32	40	15360	0	0.00	0.11	0.00
12	32	85	32640	3	0.00	0.11	0.00
13	32	75	28800	21	0.00	0.11	0.01
14	32	60	23040	84	0.00	0.11	0.03
15	32	45	17280	41	0.00	0.11	0.02
16	32	45	17280	100	0.01	0.11	0.05
17	32	60	23040	124	0.01	0.11	0.05
18	32	60	23040	82	0.00	0.11	0.03
19	32	60	23040	51	0.00	0.11	0.02
20	32	60	23040	20	0.00	0.11	0.01
21	32	60	23040	4	0.00	0.11	0.00
22	32	40	15360	0	0.00	0.11	0.00
23	32	40	15360	0	0.00	0.11	0.00
24	32	40	15360	0	0.00	0.11	0.00
25	32	40	15360	0	0.00	0.11	0.00
26	32	40	15360	0	0.00	0.11	0.00
27	32	40	15360	0	0.00	0.11	0.00
28	32	40	15360	0	0.00	0.11	0.00
29	32	40	15360	0	0.00	0.11	0.00
30	32	40	15360	0	0.00	0.11	0.00
31	32	60	23040	32	0.00	0.11	0.01
32	32	60	23040	124	0.01	0.11	0.05
33	32	45	17280	124	0.01	0.11	0.07
34	32	45	17280	20	0.00	0.11	0.01
35	32	60	23040	33	0.00	0.11	0.01
36	32	60	23040	5	0.00	0.11	0.00
37	32	60	23040	54	0.00	0.11	0.02
38	32	60	23040	32	0.00	0.11	0.01
39	32	40	15360	0	0.00	0.11	0.00
40	32	40	15360	0	0.00	0.11	0.00
41	32	40	15360	0	0.00	0.11	0.00
42	32	40	15360	0	0.00	0.11	0.00
43	32	40	15360	0	0.00	0.11	0.00
44	32	40	15360	0	0.00	0.11	0.00
45	32	40	15360	0	0.00	0.11	0.00
46	32	40	15360	0	0.00	0.11	0.00
47	32	40	15360	0	0.00	0.11	0.00
48	32	40	15360	0	0.00	0.11	0.00
49	32	30	11520	112	0.01	0.11	0.09
50	32	30	11520	140	0.01	0.11	0.11
51	32	30	11520	520	0.05	0.11	0.41
52	32	30	11520	401	0.03	0.11	0.32
53	32	30	11520	344	0.03	0.11	0.27
54	32	30	11520	406	0.04	0.11	0.32
55	32	30	11520	500	0.04	0.11	0.39
56	32	45	17280	307	0.02	0.11	0.16
57	32	45	17280	18	0.00	0.11	0.01
58	40	40	19200	0	0.00	0.11	0.00

TABLE 4 (CONTINUED)

MEMBER NUMBER	DEPTH h INCHES	WIDTH b FEET	SHEAR AREA IN-2	SHEAR FORCE KIPS	SHEAR STRESS KSI	ALLOWABLE SHEAR STRESS	SHEAR STRESS RATIO
59	40	40	19200	0	0.00	0.11	0.00
60	40	40	19200	0	0.00	0.11	0.00
61	40	40	19200	0	0.00	0.11	0.00
62	40	40	19200	0	0.00	0.11	0.00
63	40	40	19200	0	0.00	0.11	0.00
64	40	40	19200	0	0.00	0.11	0.00
65	40	40	19200	0	0.00	0.11	0.00
66	40	40	19200	0	0.00	0.11	0.00
67	40	40	19200	0	0.00	0.11	0.00
68	40	30	14400	1510	0.10	0.11	0.95
69	40	23	10800	274	0.03	0.11	0.23
70	40	15	7200	3	0.00	0.11	0.00
71	40	23	10800	261	0.02	0.11	0.22
72	40	30	14400	226	0.02	0.11	0.14
73	40	30	14400	183	0.01	0.11	0.12
74	40	23	10800	475	0.04	0.11	0.40
75	40	15	7200	327	0.05	0.11	0.41
76	40	23	10800	1485	0.14	0.11	1.25
77	40	40	19200	0	0.00	0.11	0.00
78	40	40	19200	0	0.00	0.11	0.00
79	40	40	19200	0	0.00	0.11	0.00
80	40	40	19200	0	0.00	0.11	0.00
81	40	40	19200	0	0.00	0.11	0.00
82	40	40	19200	0	0.00	0.11	0.00
83	40	40	19200	0	0.00	0.11	0.00
84	40	40	19200	0	0.00	0.11	0.00
85	40	15	7200	307	0.04	0.11	0.39
86	40	15	7200	0	0.00	0.11	0.00
87	40	23	10800	353	0.03	0.11	0.30
88	40	30	14400	189	0.01	0.11	0.12
89	40	30	14400	123	0.01	0.11	0.08
90	40	23	10800	416	0.04	0.11	0.35
91	40	23	10800	1717	0.16	0.11	1.45
92	40	40	19200	0	0.00	0.11	0.00
93	40	40	19200	0	0.00	0.11	0.00
94	40	40	19200	0	0.00	0.11	0.00
95	40	40	19200	0	0.00	0.11	0.00
96	40	40	19200	0	0.00	0.11	0.00
97	40	40	19200	0	0.00	0.11	0.00
98	40	40	19200	0	0.00	0.11	0.00
99	40	40	19200	0	0.00	0.11	0.00
100	40	40	19200	0	0.00	0.11	0.00
101	40	40	19200	0	0.00	0.11	0.00
102	40	15	7200	1394	0.19	0.11	1.76
103	40	15	7200	644	0.09	0.11	0.81
104	40	15	7200	331	0.05	0.11	0.42
105	40	15	7200	96	0.01	0.11	0.12
106	40	15	7200	354	0.05	0.11	0.45
107	40	15	7200	262	0.04	0.11	0.33
108	40	15	7200	162	0.02	0.11	0.20
109	40	15	7200	61	0.01	0.11	0.08
110	40	15	7200	236	0.03	0.11	0.30
111	40	15	7200	167	0.02	0.11	0.21
112	40	40	19200	0	0.00	0.11	0.00
113	40	40	19200	0	0.00	0.11	0.00
114	40	40	19200	0	0.00	0.11	0.00
115	40	40	19200	0	0.00	0.11	0.00
116	40	40	19200	0	0.00	0.11	0.00
117	40	40	19200	0	0.00	0.11	0.00
118	40	40	19200	0	0.00	0.11	0.00
119	40	40	19200	0	0.00	0.11	0.00

TABLE 4 (CONTINUED)

MEMBER NUMBER	DEPTH h INCHES	WIDTH b FEET	SHEAR AREA IN-2	SHEAR FORCE KIPS	SHEAR STRESS KSI	ALLOWABLE SHEAR STRESS	SHEAR STRESS RATIO
120	40	40	19200	0	0.00	0.11	0.00
121	40	15	7200	3480	0.48	0.11	4.39
122	40	15	7200	1240	0.17	0.11	1.57
123	40	15	7200	1083	0.15	0.11	1.37
124	40	15	7200	230	0.03	0.11	0.29
125	40	15	7200	626	0.09	0.11	0.79
126	40	15	7200	338	0.05	0.11	0.43
127	40	15	7200	173	0.02	0.11	0.22
128	40	15	7200	148	0.02	0.11	0.19
129	40	40	19200	0	0.00	0.11	0.00
130	40	40	19200	0	0.00	0.11	0.00
131	40	40	19200	0	0.00	0.11	0.00
132	40	40	19200	0	0.00	0.11	0.00
133	40	40	19200	0	0.00	0.11	0.00
134	40	40	19200	0	0.00	0.11	0.00
135	40	40	19200	0	0.00	0.11	0.00
136	40	15	7200	4151	0.58	0.11	5.24
137	40	15	7200	1978	0.27	0.11	2.50
138	40	15	7200	811	0.11	0.11	1.02
139	40	15	7200	567	0.08	0.11	0.72
140	40	15	7200	370	0.05	0.11	0.47
141	40	15	7200	160	0.02	0.11	0.20
142	40	40	19200	0	0.00	0.11	0.00
143	40	40	19200	0	0.00	0.11	0.00
144	40	40	19200	0	0.00	0.11	0.00
145	40	40	19200	0	0.00	0.11	0.00
146	40	40	19200	0	0.00	0.11	0.00
147	40	15	7200	141	0.02	0.11	0.18
148	40	15	7200	45	0.01	0.11	0.06
149	40	15	7200	385	0.05	0.11	0.49
150	40	15	7200	1037	0.14	0.11	1.31
151	40	30	14400	0	0.00	0.11	0.00
152	40	30	14400	0	0.00	0.11	0.00
153	40	30	14400	0	0.00	0.11	0.00
154	40	30	14400	0	0.00	0.11	0.00
155	40	30	14400	0	0.00	0.11	0.00
156	40	15	7200	4072	0.57	0.11	5.14
157	40	15	7200	4335	0.60	0.11	5.47
158	40	15	7200	5177	0.72	0.11	6.54
159	40	15	7200	4481	0.62	0.11	5.66

TABLE 5

FLEXURE: CONGLOMERATE SHELL--PANEL JOINTS RELEASED

MEMBER NUMBER	DEPTH h INCHES	WIDTH b FEET	SECTION MODULUS IN-3	BENDING MOMENT IN-KIPS	FLEXURAL STRESS KSI	ALLOWABLE FLEXURAL STRESS	FLEXURAL STRESS RATIO
1	32	40	81920	0	0.00	0.41	0.00
2	32	40	81920	0	0.00	0.41	0.00
3	32	40	81920	0	0.00	0.41	0.00
4	32	40	81920	0	0.00	0.41	0.00
5	32	40	81920	0	0.00	0.41	0.00
6	32	40	81920	0	0.00	0.41	0.00
7	32	40	81920	0	0.00	0.41	0.00
8	32	40	81920	0	0.00	0.41	0.00
9	32	40	81920	0	0.00	0.41	0.00
10	32	40	81920	0	0.00	0.41	0.00
11	32	40	81920	0	0.00	0.41	0.00
12	32	85	174080	145	0.00	0.41	0.00
13	32	75	153600	2745	0.02	0.41	0.04
14	32	60	122880	16120	0.13	0.41	0.32
15	32	45	92160	33960	0.37	0.41	0.90
16	32	45	92160	45840	0.50	0.41	1.21
17	32	60	122880	58700	0.48	0.41	1.17
18	32	60	122880	37310	0.30	0.41	0.74
19	32	60	122880	14590	0.12	0.41	0.29
20	32	60	122880	3803	0.03	0.41	0.08
21	32	60	122880	367	0.00	0.41	0.01
22	32	40	81920	0	0.00	0.41	0.00
23	32	40	81920	0	0.00	0.41	0.00
24	32	40	81920	0	0.00	0.41	0.00
25	32	40	81920	0	0.00	0.41	0.00
26	32	40	81920	0	0.00	0.41	0.00
27	32	40	81920	0	0.00	0.41	0.00
28	32	40	81920	0	0.00	0.41	0.00
29	32	40	81920	0	0.00	0.41	0.00
30	32	40	81920	0	0.00	0.41	0.00
31	32	60	122880	8362	0.07	0.41	0.17
32	32	60	122880	31790	0.26	0.41	0.63
33	32	45	92160	63590	0.69	0.41	1.68
34	32	45	92160	63850	0.69	0.41	1.69
35	32	60	122880	83420	0.68	0.41	1.66
36	32	60	122880	44210	0.36	0.41	0.88
37	32	60	122880	24630	0.20	0.41	0.49
38	32	60	122880	11040	0.09	0.41	0.22
39	32	40	81920	0	0.00	0.41	0.00
40	32	40	81920	0	0.00	0.41	0.00
41	32	40	81920	0	0.00	0.41	0.00
42	32	40	81920	0	0.00	0.41	0.00
43	32	40	81920	0	0.00	0.41	0.00
44	32	40	81920	0	0.00	0.41	0.00
45	32	40	81920	0	0.00	0.41	0.00
46	32	40	81920	0	0.00	0.41	0.00
47	32	40	81920	0	0.00	0.41	0.00
48	32	40	81920	0	0.00	0.41	0.00
49	32	30	61440	31230	0.51	0.41	1.24
50	32	30	61440	86500	1.41	0.41	3.43
51	32	30	61440	129800	2.11	0.41	5.15
52	32	30	61440	89670	1.46	0.41	3.56
53	32	30	61440	90100	1.47	0.41	3.58
54	32	30	61440	91900	1.50	0.41	3.65
55	32	30	61440	132600	2.16	0.41	5.26
56	32	45	92160	149300	1.62	0.41	3.95
57	32	45	92160	32690	0.35	0.41	0.87
58	40	40	128000	0	0.00	0.41	0.00

TABLE 5 (CONTINUED)

MEMBER NUMBER	DEPTH h INCHES	WIDTH b FEET	SECTION MODULUS IN-3	BENDING MOMENT IN-KIPS	FLEXURAL STRESS KSI	ALLOWABLE FLEXURAL STRESS	FLEXURAL STRESS RATIO
59	40	40	128000	0	0.00	0.41	0.00
60	40	40	128000	0	0.00	0.41	0.00
61	40	40	128000	0	0.00	0.41	0.00
62	40	40	128000	0	0.00	0.41	0.00
63	40	40	128000	0	0.00	0.41	0.00
64	40	40	128000	0	0.00	0.41	0.00
65	40	40	128000	0	0.00	0.41	0.00
66	40	40	128000	0	0.00	0.41	0.00
67	40	40	128000	0	0.00	0.41	0.00
68	40	30	96000	334100	3.48	0.41	8.49
69	40	23	72000	100300	1.39	0.41	3.40
70	40	15	48000	28110	0.59	0.41	1.43
71	40	23	72000	75840	1.05	0.41	2.57
72	40	30	96000	65540	0.68	0.41	1.67
73	40	30	96000	82250	0.86	0.41	2.09
74	40	23	72000	139500	1.94	0.41	4.73
75	40	15	48000	85850	1.79	0.41	4.36
76	40	23	72000	335000	4.65	0.41	11.35
77	40	40	128000	0	0.00	0.41	0.00
78	40	40	128000	0	0.00	0.41	0.00
79	40	40	128000	0	0.00	0.41	0.00
80	40	40	128000	0	0.00	0.41	0.00
81	40	40	128000	0	0.00	0.41	0.00
82	40	40	128000	0	0.00	0.41	0.00
83	40	40	128000	0	0.00	0.41	0.00
84	40	40	128000	0	0.00	0.41	0.00
85	40	15	48000	75950	1.58	0.41	3.86
86	40	15	48000	48720	1.02	0.41	2.48
87	40	23	72000	96060	1.33	0.41	3.25
88	40	30	96000	47730	0.50	0.41	1.21
89	40	30	96000	25590	0.27	0.41	0.65
90	40	23	72000	74640	1.04	0.41	2.53
91	40	23	72000	331500	4.60	0.41	11.23
92	40	40	128000	0	0.00	0.41	0.00
93	40	40	128000	0	0.00	0.41	0.00
94	40	40	128000	0	0.00	0.41	0.00
95	40	40	128000	0	0.00	0.41	0.00
96	40	40	128000	0	0.00	0.41	0.00
97	40	40	128000	0	0.00	0.41	0.00
98	40	40	128000	0	0.00	0.41	0.00
99	40	40	128000	0	0.00	0.41	0.00
100	40	40	128000	0	0.00	0.41	0.00
101	40	40	128000	0	0.00	0.41	0.00
102	40	15	48000	286400	5.97	0.41	14.55
103	40	15	48000	139200	2.90	0.41	7.07
104	40	15	48000	142100	2.96	0.41	7.22
105	40	15	48000	89790	1.87	0.41	4.56
106	40	15	48000	90110	1.88	0.41	4.58
107	40	15	48000	49490	1.03	0.41	2.51
108	40	15	48000	20430	0.43	0.41	1.04
109	40	15	48000	11090	0.23	0.41	0.56
110	40	15	48000	44610	0.93	0.41	2.27
111	40	15	48000	62910	1.31	0.41	3.20
112	40	40	128000	0	0.00	0.41	0.00
113	40	40	128000	0	0.00	0.41	0.00
114	40	40	128000	0	0.00	0.41	0.00
115	40	40	128000	0	0.00	0.41	0.00
116	40	40	128000	0	0.00	0.41	0.00
117	40	40	128000	0	0.00	0.41	0.00
118	40	40	128000	0	0.00	0.41	0.00
119	40	40	128000	0	0.00	0.41	0.00

TABLE 5 (CONTINUED)

MEMBER NUMBER	DEPTH h INCHES	WIDTH b FEET	SECTION MODULUS IN-3	BENDING MOMENT IN-KIPS	FLEXURAL STRESS KSI	ALLOWABLE FLEXURAL STRESS	FLEXURAL STRESS RATIO
120	40	40	128000	0	0.00	0.41	0.00
121	40	15	48000	353200	7.36	0.41	17.95
122	40	15	48000	217300	4.53	0.41	11.04
123	40	15	48000	196900	4.10	0.41	10.01
124	40	15	48000	115200	2.40	0.41	5.85
125	40	15	48000	121500	2.53	0.41	6.17
126	40	15	48000	57060	1.19	0.41	2.90
127	40	15	48000	28580	0.60	0.41	1.45
128	40	15	48000	23670	0.49	0.41	1.20
129	40	40	128000	0	0.00	0.41	0.00
130	40	40	128000	0	0.00	0.41	0.00
131	40	40	128000	0	0.00	0.41	0.00
132	40	40	128000	0	0.00	0.41	0.00
133	40	40	128000	0	0.00	0.41	0.00
134	40	40	128000	0	0.00	0.41	0.00
135	40	40	128000	0	0.00	0.41	0.00
136	40	15	48000	238500	4.97	0.41	12.12
137	40	15	48000	369900	7.71	0.41	18.80
138	40	15	48000	142700	2.97	0.41	7.25
139	40	15	48000	113300	2.36	0.41	5.76
140	40	15	48000	96630	2.01	0.41	4.91
141	40	15	48000	70930	1.48	0.41	3.60
142	40	40	128000	0	0.00	0.41	0.00
143	40	40	128000	0	0.00	0.41	0.00
144	40	40	128000	0	0.00	0.41	0.00
145	40	40	128000	0	0.00	0.41	0.00
146	40	40	128000	0	0.00	0.41	0.00
147	40	15	48000	174900	3.64	0.41	8.89
148	40	15	48000	183700	3.83	0.41	9.33
149	40	15	48000	127900	2.66	0.41	6.50
150	40	15	48000	226500	4.72	0.41	11.51
151	40	30	96000	0	0.00	0.41	0.00
152	40	30	96000	0	0.00	0.41	0.00
153	40	30	96000	0	0.00	0.41	0.00
154	40	30	96000	0	0.00	0.41	0.00
155	40	30	96000	0	0.00	0.41	0.00
156	40	15	48000	400700	8.35	0.41	20.36
157	40	15	48000	358800	7.48	0.41	18.23
158	40	15	48000	325500	6.78	0.41	16.54
159	40	15	48000	251400	5.24	0.41	12.77

TABLE 6

SHEAR: CONGLOMERATE SHELL--PANEL JOINTS RELEASED

MEMBER NUMBER	DEPTH h INCHES	WIDTH b FEET	SHEAR AREA IN-2	SHEAR FORCE KIPS	SHEAR STRESS KSI	ALLOWABLE SHEAR STRESS	SHEAR STRESS RATIO
1	32	40	15360	0	0.00	0.11	0.00
2	32	40	15360	0	0.00	0.11	0.00
3	32	40	15360	0	0.00	0.11	0.00
4	32	40	15360	0	0.00	0.11	0.00
5	32	40	15360	0	0.00	0.11	0.00
6	32	40	15360	0	0.00	0.11	0.00
7	32	40	15360	0	0.00	0.11	0.00
8	32	40	15360	0	0.00	0.11	0.00
9	32	40	15360	0	0.00	0.11	0.00
10	32	40	15360	0	0.00	0.11	0.00
11	32	40	15360	0	0.00	0.11	0.00
12	32	85	32640	0	0.00	0.11	0.00
13	32	75	28800	10	0.00	0.11	0.00
14	32	60	23040	54	0.00	0.11	0.02
15	32	45	17280	47	0.00	0.11	0.02
16	32	45	17280	93	0.01	0.11	0.05
17	32	60	23040	116	0.01	0.11	0.05
18	32	60	23040	71	0.00	0.11	0.03
19	32	60	23040	40	0.00	0.11	0.02
20	32	60	23040	13	0.00	0.11	0.01
21	32	60	23040	0	0.00	0.11	0.00
22	32	40	15360	0	0.00	0.11	0.00
23	32	40	15360	0	0.00	0.11	0.00
24	32	40	15360	0	0.00	0.11	0.00
25	32	40	15360	0	0.00	0.11	0.00
26	32	40	15360	0	0.00	0.11	0.00
27	32	40	15360	0	0.00	0.11	0.00
28	32	40	15360	0	0.00	0.11	0.00
29	32	40	15360	0	0.00	0.11	0.00
30	32	40	15360	0	0.00	0.11	0.00
31	32	60	23040	20	0.00	0.11	0.01
32	32	60	23040	90	0.00	0.11	0.04
33	32	45	17280	69	0.00	0.11	0.04
34	32	45	17280	31	0.00	0.11	0.02
35	32	60	23040	28	0.00	0.11	0.01
36	32	60	23040	1	0.00	0.11	0.00
37	32	60	23040	47	0.00	0.11	0.02
38	32	60	23040	27	0.00	0.11	0.01
39	32	40	15360	0	0.00	0.11	0.00
40	32	40	15360	0	0.00	0.11	0.00
41	32	40	15360	0	0.00	0.11	0.00
42	32	40	15360	0	0.00	0.11	0.00
43	32	40	15360	0	0.00	0.11	0.00
44	32	40	15360	0	0.00	0.11	0.00
45	32	40	15360	0	0.00	0.11	0.00
46	32	40	15360	0	0.00	0.11	0.00
47	32	40	15360	0	0.00	0.11	0.00
48	32	40	15360	0	0.00	0.11	0.00
49	32	30	11520	77	0.01	0.11	0.06
50	32	30	11520	185	0.02	0.11	0.15
51	32	30	11520	438	0.04	0.11	0.35
52	32	30	11520	311	0.03	0.11	0.25
53	32	30	11520	292	0.03	0.11	0.23
54	32	30	11520	315	0.03	0.11	0.25
55	32	30	11520	424	0.04	0.11	0.33
56	32	45	17280	339	0.02	0.11	0.18
57	32	45	17280	41	0.00	0.11	0.02
58	40	40	19200	200	0.01	0.11	0.09

TABLE 6 (CONTINUED)

MEMBER NUMBER	DEPTH h INCHES	WIDTH b FEET	SHEAR AREA IN-2	SHEAR FORCE KIPS	SHEAR STRESS KSI	ALLOWABLE SHEAR STRESS	SHEAR STRESS RATIO
59	40	40	19200	0	0.00	0.11	0.00
60	40	40	19200	0	0.00	0.11	0.00
61	40	40	19200	0	0.00	0.11	0.00
62	40	40	19200	0	0.00	0.11	0.00
63	40	40	19200	0	0.00	0.11	0.00
64	40	40	19200	0	0.00	0.11	0.00
65	40	40	19200	0	0.00	0.11	0.00
66	40	40	19200	0	0.00	0.11	0.00
67	40	40	19200	0	0.00	0.11	0.00
68	40	30	14400	1279	0.09	0.11	0.81
69	40	23	10800	235	0.02	0.11	0.20
70	40	15	7200	5	0.00	0.11	0.01
71	40	23	10800	146	0.01	0.11	0.12
72	40	30	14400	40	0.00	0.11	0.03
73	40	30	14400	95	0.01	0.11	0.06
74	40	23	10800	366	0.03	0.11	0.31
75	40	15	7200	188	0.03	0.11	0.24
76	40	23	10800	1219	0.11	0.11	1.03
77	40	40	19200	0	0.00	0.11	0.00
78	40	40	19200	0	0.00	0.11	0.00
79	40	40	19200	0	0.00	0.11	0.00
80	40	40	19200	0	0.00	0.11	0.00
81	40	40	19200	0	0.00	0.11	0.00
82	40	40	19200	0	0.00	0.11	0.00
83	40	40	19200	0	0.00	0.11	0.00
84	40	40	19200	0	0.00	0.11	0.00
85	40	15	7200	160	0.02	0.11	0.20
86	40	15	7200	48	0.01	0.11	0.06
87	40	23	10800	219	0.02	0.11	0.18
88	40	30	14400	67	0.00	0.11	0.04
89	40	30	14400	35	0.00	0.11	0.02
90	40	23	10800	301	0.03	0.11	0.25
91	40	23	10800	1320	0.12	0.11	1.11
92	40	40	19200	0	0.00	0.11	0.00
93	40	40	19200	0	0.00	0.11	0.00
94	40	40	19200	0	0.00	0.11	0.00
95	40	40	19200	0	0.00	0.11	0.00
96	40	40	19200	0	0.00	0.11	0.00
97	40	40	19200	0	0.00	0.11	0.00
98	40	40	19200	0	0.00	0.11	0.00
99	40	40	19200	0	0.00	0.11	0.00
100	40	40	19200	0	0.00	0.11	0.00
101	40	40	19200	0	0.00	0.11	0.00
102	40	15	7200	1044	0.15	0.11	1.32
103	40	15	7200	326	0.05	0.11	0.41
104	40	15	7200	326	0.05	0.11	0.41
105	40	15	7200	162	0.02	0.11	0.20
106	40	15	7200	251	0.03	0.11	0.32
107	40	15	7200	155	0.02	0.11	0.20
108	40	15	7200	70	0.01	0.11	0.09
109	40	15	7200	32	0.00	0.11	0.04
110	40	15	7200	144	0.02	0.11	0.18
111	40	15	7200	165	0.02	0.11	0.21
112	40	40	19200	0	0.00	0.11	0.00
113	40	40	19200	0	0.00	0.11	0.00
114	40	40	19200	0	0.00	0.11	0.00
115	40	40	19200	0	0.00	0.11	0.00
116	40	40	19200	0	0.00	0.11	0.00
117	40	40	19200	0	0.00	0.11	0.00
118	40	40	19200	0	0.00	0.11	0.00
119	40	40	19200	0	0.00	0.11	0.00

TABLE 6 (CONTINUED)

MEMBER NUMBER	DEPTH h INCHES	WIDTH b FEET	SHEAR AREA IN-2	SHEAR FORCE KIPS	SHEAR STRESS KSI	ALLOWABLE SHEAR STRESS	SHEAR STRESS RATIO
120	40	40	19200	0	0.00	0.11	0.00
121	40	15	7200	2874	0.40	0.11	3.63
122	40	15	7200	855	0.12	0.11	1.08
123	40	15	7200	669	0.09	0.11	0.84
124	40	15	7200	303	0.04	0.11	0.38
125	40	15	7200	418	0.06	0.11	0.53
126	40	15	7200	192	0.03	0.11	0.24
127	40	15	7200	90	0.01	0.11	0.11
128	40	15	7200	70	0.01	0.11	0.09
129	40	40	19200	0	0.00	0.11	0.00
130	40	40	19200	0	0.00	0.11	0.00
131	40	40	19200	0	0.00	0.11	0.00
132	40	40	19200	0	0.00	0.11	0.00
133	40	40	19200	0	0.00	0.11	0.00
134	40	40	19200	0	0.00	0.11	0.00
135	40	40	19200	0	0.00	0.11	0.00
136	40	15	7200	3641	0.51	0.11	4.60
137	40	15	7200	1431	0.20	0.11	1.81
138	40	15	7200	584	0.08	0.11	0.74
139	40	15	7200	388	0.05	0.11	0.49
140	40	15	7200	270	0.04	0.11	0.34
141	40	15	7200	147	0.02	0.11	0.19
142	40	40	19200	0	0.00	0.11	0.00
143	40	40	19200	0	0.00	0.11	0.00
144	40	40	19200	0	0.00	0.11	0.00
145	40	40	19200	0	0.00	0.11	0.00
146	40	40	19200	0	0.00	0.11	0.00
147	40	15	7200	333	0.05	0.11	0.42
148	40	15	7200	272	0.04	0.11	0.34
149	40	15	7200	48	0.01	0.11	0.06
150	40	15	7200	562	0.08	0.11	0.71
151	40	30	14400	0	0.00	0.11	0.00
152	40	30	14400	0	0.00	0.11	0.00
153	40	30	14400	0	0.00	0.11	0.00
154	40	30	14400	0	0.00	0.11	0.00
155	40	30	14400	0	0.00	0.11	0.00
156	40	15	7200	3199	0.44	0.11	4.04
157	40	15	7200	3538	0.49	0.11	4.47
158	40	15	7200	4437	0.62	0.11	5.60
159	40	15	7200	3840	0.53	0.11	4.85

VITA

E. Wayne Kutch

Candidate for the Degree of

Master of Science

Thesis: A DEFORMATION ANALYSIS OF THE SEEPAGE CUTOFF WALL AT MUD MOUNTAIN DAM, WASHINGTON

Major Field: Civil Engineering

Biographical:

Personal Data: Born in Seattle, Washington, July 10, 1955, the son of Edward W. and Lillian P. Kutch.

Education: Graduated from Highline High School, Seattle, Washington, in June, 1973; received the Bachelor of Science degree in Civil Engineering from the University of Washington, Seattle, Washington, in March, 1979; completed requirements for the Master of Science degree at Oklahoma State University in May, 1991.

Professional Experience: Civil Engineer, U.S. Army Corps of Engineers, Seattle District, November, 1979, to March, 1981; Engineer-in-Training, U.S. Army Corps of Engineers, March, 1981, to March, 1982; Structural Engineer, U.S. Army Corps of Engineers, Seattle District, March, 1982, to August, 1989.

Professional Affiliations: Washington State Registered Professional Engineer, 1984; member of the American Society of Civil Engineers.